Forest Ecology and Management 554 (2024) 121659

Contents lists available at ScienceDirect

Forest Ecology and Management

journal homepage: www.elsevier.com/locate/foreco

Threats to the persistence of sugar pine (*Pinus lambertiana*) in the western USA

Daniel E. Foster *, Scott S. Stephens, Perry de Valpine, John J. Battles

University of California, Berkeley, Department of Environmental Science, Policy and Management, 130 Mulford Hall #3114, Berkeley, CA 94720-3114, United States

ARTICLE INFO

Keywords:
Fire
Drought
Pathogens
Demography
Integral projection models

ABSTRACT

This study assesses how numerous stressors shape the vital rates (survival, growth, and fecundity) of sugar pine across the vast majority of its range. Sugar pine (*Pinus lambertiana* Dougl.) is the largest Pinus species, an important timber species, and a component of several dry conifer forest types of western North America, in particular the extensive Sierra Nevada mixed conifer forest. The species faces several challenges in the Anthropocene, including a disrupted fire regime, an invasive pathogen, forest structure changes, and drought with ensuing bark beetle epidemics. Managers are concerned about the conservation outlook for sugar pine, but it is unclear where and how to best invest conservation resources. Using data from the US Forest Service's Forest Inventory and Analysis program, we estimate the parameters for the vital rate functions and use these to construct an integral projection model which predicts the effects of various stressors on the asymptotic population growth rate. The asymptotic population growth rate is near or slightly below one even under reference conditions, and the actual abundance (in terms of both stem density and basal area) slightly declined over the duration of the study (2001–2019). The analysis reveals that wildfire, white pine blister rust, and forest density are key drivers of the demographic rates of sugar pine across its range. Drought and site dryness had lesser, but still meaningful, effects. Fire has strong negative effects on survival, resulting in a strongly negative population trajectory on burned sites. Conversely, lower than average forest density (plot-level basal area) results in a positive population growth rate via beneficial effects on individual growth. These results highlight the value of fire hazard mitigation, particularly where it also reduces forest density, in the conservation of this important species.

1. Introduction

1.1. Overview

The ecology of the Anthropocene is characterized by the global loss of biodiversity, the emergence of novel disturbance regimes, and the degradation of ecosystem services (Bradshaw et al., 2021; Kress and Krupnick, 2022; Millar et al., 2007; Newman, 2019). Trees and forests are no exception. Almost a third (30%) of the extent tree species are at risk of extinction (BGCI, 2021). A decline in tree biodiversity at this scale jeopardizes the sustainability of forest ecosystems and the well-being of human livelihoods (Rivers et al., 2023).

An immediate management need is to assess the threats to tree species. Globally, forest conversion for development or agriculture represents the primary driver of tree extinctions (BGCI, 2021). But in North America, invasive pests and pathogens along with climate change are the major hazards (Rivers et al., 2023). For fire-prone forest, the disruption of the fire regime also poses a significant challenge to biodiversity conservation (Spies et al., 2012).

In the western United States, there has been a long-standing concern about the persistence of sugar pine (*Pinus lambertiana* Dougl., Kinloch et al., 1996). Sugar pine faces a suite of novel stressors including an invasive pathogen, hotter droughts, and an altered fire regime (van Mantgem et al., 2004; Maloney et al., 2011; Dudney et al., 2020). However, despite the perception of resource professionals and public stakeholders "that sugar pine as a species might be in imminent jeopardy" (Kinloch and Marosy, 1996), global and national assessments do not consider sugar pine a species currently at risk of extinction. NatureServe classifies the conservation status of sugar pine as "secure" (NatureServe, 2023); the International Union for Conservation of Nature (IUCN) Red List describes it as a species of "Least Concern" (IUCN, 2022); and Stanke et al.'s (2020) forest stability index ranks sugar pine

* Corresponding author.
E-mail address: danielfoster1787@gmail.com (D.E. Foster).

https://doi.org/10.1016/j.foreco.2023.121659
Received 19 August 2023; Received in revised form 14 December 2023; Accepted 17 December 2023
Available online 6 January 2024

as a stable tree species (i.e., not in decline). Moreover, a recent review of plants likely to be winners and losers in the Anthropocene identifies sugar pine as a "winner useful to humans" (Kress and Krupnick, 2022). Even detailed, site-specific studies conducted of sugar pine populations exposed to known stressors do not report consistent evidence of decline (van Mantgem et al., 2004; Maloney et al., 2011).

This contrast between perception and evidence presents a major challenge to forest management. To date, efforts to protect sugar pine have been extensive (e.g., Aitken and Whitlock, 2013; Waring and Goodrich, 2012, Stevens et al., 2016, Hood et al., 2022, Sniezko and Liu, 2022). And yet, resources for conservation and restoration are limited. These scarce resources must be prioritized given the broad risks posed by novel anthropogenic stressors (Millar et al., 2007).

In this paper, we evaluated the status of sugar pine and quantified the vulnerability of sugar pine to major stressors. Specifically, we addressed four questions:

1) What are the recent changes in sugar pine abundance across its range?
2) What are the regional differences in the trajectory of sugar pine populations across its range?
3) What is the relative importance of the major stressors on sugar pine vital rates?
4) What is the likely impact of these stressors on sugar pine population dynamics?

To answer these questions, we took advantage of data from the U.S. Forest Service Forest Inventory and Assessment Program (FIA, Burrill et al., 2021, Westfall et al., 2022). First, we conducted a range-wide assessment of sugar pine population decline between 2010 and 2019 (*sensu* Stanke et al., 2020). Next, we used the FIA data to estimate vital rates as a function of individual size and the presence or severity of potential stressors (Eitzel et al., 2013, 2015; Kohyama et al., 2018; Shriver et al., 2021). Once the impacts of stressors on individual vital rates were quantified, we predicted the population trajectory in response to each stressor by synthesizing the vital rates in an integral projection model (IPM; Merow et al., 2014; Needham et al., 2018; Doak et al., 2021). Our overarching goal was to quantify the threats to sugar pine persistence in order to inform sugar pine management.

1.2. Background

Sugar pine is the largest pine species in both height and volume; it is an important timber species; and it is a component of several dry western conifer forest types (Kinloch and Scheuner, 1990). In the extensive Sierra Nevada mixed conifer forest, sugar pine typically comprises 5–25% of basal area (Safford and Stevens, 2017; Bohlman et al., 2021). Its range extends through much of the North American Mediterranean zone throughout mountain ranges in California and central Oregon. There is a small population in northwestern Mexico but California encompasses the heart of its range (Kinloch and Scheuner, 1990). Sugar pine seeds are an important food source for animal species (Fowells and Schubert, 1956; Thayer et al., 2005; Murray and Tomback, 2010), and mature sugar pines are large-diameter trees which play a key role in the structure and function of ecosystems in which they occur (Lutz, 2018; Lutz et al., 2013, 2020). However, sugar pine trees face numerous challenges in the Anthropocene.

First, disruptions to the fire regime impact the fitness of this moderately shade-tolerant, fire-surviving species (Schwilk and Ackerly, 2001; Niinemets and Valladares, 2006). In California, sugar pine reaches its greatest dominance in frequent fire forest types with mean fire return intervals of at most 11–16 years (Yeaton, 1983, 1984; Safford and Stevens, 2017; Bohlman et al., 2021). Large adults typically survive low-to-moderate severity wildfires and produce recruits that can take advantage of the reduced competition for light and water in the post-fire environment. However, changes in forest structure wrought by historical timber harvests and fire suppression, coupled with a warming climate, have increased sugar pine's exposure to high severity wildfire (Safford and Stevens, 2017; Stevens et al., 2017; Parks and Abatzoglou, 2020; Bohlman et al., 2021). This altered fire regime threatens not only the persistence of sugar pine but also the mixed conifer forest type as a whole (Steel et al., 2015; Shive et al., 2018; Coop et al., 2020).

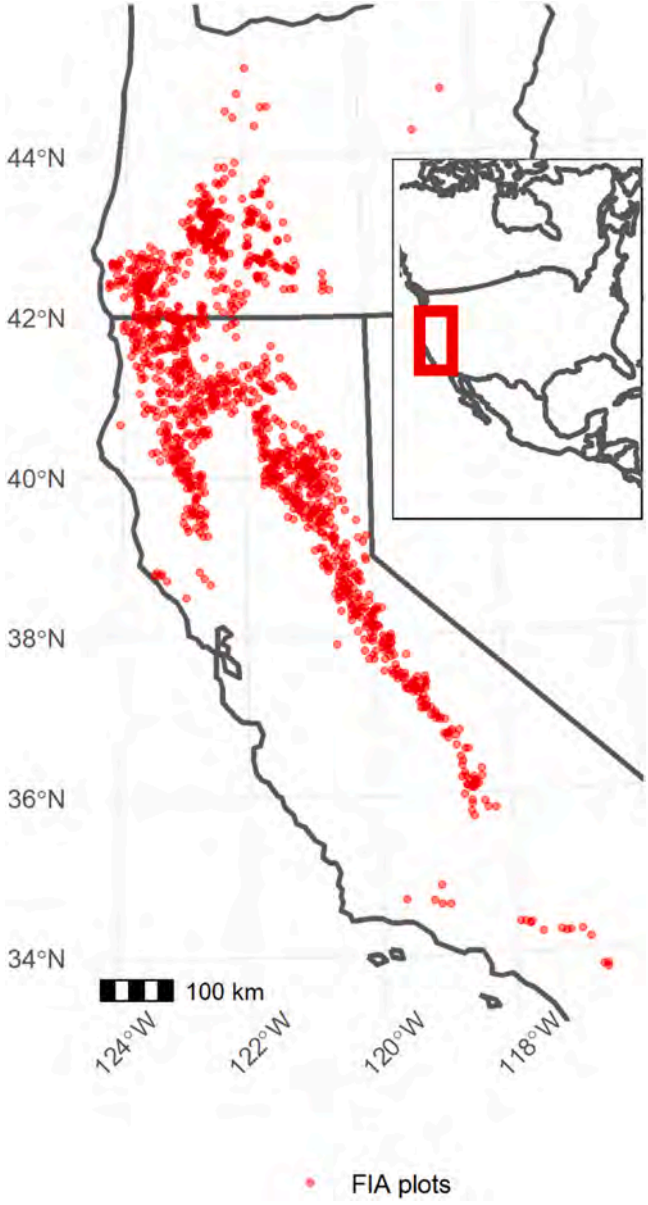

Fig. 1. 1221 Forest Inventory and Analysis (FIA) plots where live sugar pine was present at initial measurement (2001–2009) or remeasurement (2010–2019) with US state borders. Plot locations based on the fuzzed, rather than true, coordinates. Inset shows position relative to North America and national borders.

Second, an invasive fungal pathogen, *Cronartium ribicola* (white pine blister rust; WPBR) has spread across much of sugar pine's range since its introduction to North America in the early 20th century, causing substantial mortality (van Mantgem et al., 2004; Maloney et al., 2011; Dudney et al., 2020). WPBR affects white pines (subgenus *Strobus*, excluding the pinyon pines in subsection *Cembroides*) by parasitizing foliage, shoots, inner bark, and outer xylem, causing the formation of cankers which can reduce vigor and kill outright by girdling the stem (Geils et al., 2010). The epidemic in the western United States has been severe enough to cause the related species, *Pinus albicaulis*, to be listed as

Endangered by ICUN (Mahalovich and Stritch, 2013) and more recently, it was listed as Threatened under the Endangered Species Act of the United States (US Fish and Wildlife Service, 2020).

Third, there is evidence that the contemporary forest structure impacts the population dynamics of sugar pine, beyond its contribution to an altered fire regime, by increasing competitive stress. Effective fire suppression, which was instituted across much of sugar pine's range in the 20th century, has resulted in an overall densification of these forests (Stephens et al., 2015; Safford and Stevens, 2017; Bohlman et al., 2021; North et al., 2022). In these dense forests, the recruitment of sugar pine is limited (van Mantgem et al., 2004) especially in comparison to the more shade-tolerant tree species (e.g., *Abies concolor* and *Calocedrus decurrens*, Ansley and Battles, 1998; Levine et al., 2016). There is also evidence that increased competition in these crowded forests has reduced the vigor of adult sugar pines, thus reducing their ability to resist other stresses (Young et al., 2017; Restaino et al., 2019; Furniss et al., 2021; North et al., 2022).

Finally, the changing climate may increase the duration and aridity of droughts and thus water stress. Heightened water stress at the landscape scale can drive bark beetle epidemics, which have already caused mass mortality events in sugar pine's range (Fettig et al., 2019; Stephenson et al., 2019; Steel et al., 2021). Once these epidemics are underway, bark beetles tend to preferentially target healthy reproductively-valuable large and sugar pines (Stephenson et al., 2019), exacerbating the impact of this pest on the demographic outlook for sugar pine. Water stress can also kill trees, especially small individuals, more directly via hydraulic failure and/or carbon starvation (Moran et al., 2019).

2. Methods

2.1. Study area

We focused on the status of sugar pine in the contiguous United States (Fig. 1). This area of interest represents the vast majority of sugar pine's range; it excludes only an isolated population in Baja California. The range of sugar pine in the United States extends from 33.7°N to 45.3°N throughout much of the Sierra Nevada and Klamath mountains, and parts of the Transverse, Peninsular, and Southern Cascades ranges in the US states of California and Oregon. Sugar pine is widely distributed throughout this range as an important element of the mixed conifer forest belt at elevations ranging from 1000 m to 2700 m (Safford and Stevens, 2017; Bohlman et al., 2021). The climate throughout this range is Mediterranean, with a cool-wet season and a warm-dry season (Safford and Stevens, 2017).

2.2. Inventory data

The Forest Inventory and Analysis program (FIA) conducts the national forest inventory program for the United States (Westfall et al., 2022). Since 2001, the empirical foundation to the national inventory consists of a network of repeat-measure, tagged-tree, fixed-area plots measured at decadal frequency in the western United States (Phase 2 plots, Westfall et al., 2022). In the public database, the geographic coordinates listed for the FIA plots are not exact. To protect privacy and preserve plot integrity, the coordinates are "fuzzed." This fuzzing includes randomly perturbing the location of all plots so that most fuzzed locations are within 0.8 km of the true location and no fuzzed location is more than 1.6 km from the true location. In addition, between 0% and 20% of plots on private land ownership have their coordinates swapped with a compositionally and structurally similar private-ownership plot in the same county (Burrill et al., 2021; Westfall et al., 2022). In our dataset, 280 out of 1221 plots were privately owned, so up to 56 (4.6%) of plots may have had their coordinates swapped. We assessed the effect of using fuzzed and swapped coordinates to extract bioclimatic variables (described below) by treating the observed values as true and simulating 1000 fuzzed and swapped datasets. The results of that analyses (Supplementary Figure 1) indicate that the error introduced by fuzzing and swapping is very small for the vast majority of plots, relative to the distribution of climate variables across plots (Supplementary Figure 2).

FIA plots are placed on a hexagonal grid with a density of approximately 1 plot per 2429 ha. Each plot is revisited approximately once every 10 years, which we treat as the census interval for the purpose of modeling population dynamics. Of the plots used for this study, 90% had an inventory interval from 9.6 to 10.3 years, with a mean interval of 10.0 years, a minimum interval of 7.9 years, and a maximum interval of 12.3 years. Each included plot was remeasured one time in this study. Thus, there is one census interval per plot, with the initial censuses taking place from 2001–2009 and the remeasurements from 2011–2019.

The design of the FIA Phase 2 tree inventory relies on both spatial adjacency and nesting to conduct a statistically robust sample of trees at each location (Burrill et al., 2021; Westfall et al., 2022). Thus, each Phase 2 plot is a constellation of fixed-area samples. Trees $\geq$ 12.7 cm diameter at breast height (DBH, breast height = 1.37 m) are inventoried on four 168 m^2 permanent subplots. Small trees from 2.54–12.7 cm DBH are inventoried on four 13.5 m^2 microplots nested within the subplots, and large trees ($\geq$ 70.0 cm or $\geq$ 91.4 cm DBH, depending on the plot) on four 1012 m^2 macroplots that include the subplot. Data inventoried for each individual stem include the species, live/dead status, DBH, and (up to) three damage agent and severity codes indicating whether some agent (e.g., white pine blister rust) is visibly affecting the individual's health. Trees (all stems $\geq$ 2.54 cm DBH) are physically tagged to facilitate relocation of specific individuals at remeasurement. In addition to the tree-level data collected, the FIA program also records information about forest conditions, including the presence of significant disturbances (e.g., fire), the ecological subsection the plot is located within (Bailey, 2016), and the fuzzed GPS coordinates of the plot center.

These repeated inventories for California and Oregon (FIA Phase 2 Database version 1.8.0.03) were first used to quantify the decadal trend in sugar pine abundance using FIA's design-based estimators (Scott et al., 2005; Stanke et al., 2020). For the demographic analyses, we selected the 1221 Phase 2 plots where live sugar pine was present in the plot at either the initial measurement (2001–2009) or first remeasurement (2010–2019). With these data, we estimated parameters for vital rate functions (described in detail below) of survival, growth, and recruitment across the range of sugar pine. The fate of 3530 sugar pine individuals was tracked to estimate the parameters of the survival function (an average of 3.3 individuals per plot); the growth of the 2821 surviving individuals was measured to estimate the growth function (an average of 3.0 individuals per plot); and the observed fecundity, namely the mean number of new recruits per existing individual, was calculated to estimate the recruitment function. Recruits were defined as stems with DBH between 2.54 cm and 12.7 cm that were not present on the microplot at initial census but appeared in the second census. This estimate of fecundity was based on the 967 plots with sugar pine present at initial census.

2.3. Climate data

To assess the water stress experienced by sugar pine individuals, we extracted monthly climatic water deficit (CWD) estimates for each fuzzed plot location from the TerraClimate dataset (Abatzoglou et al., 2018). CWD is a measure of evaporative demand not met by available water (Stephenson, 1998). The TerraClimate dataset provides modeled estimates of CWD at 4 km resolution for the years 1958–2020. The 4 km resolution approximately matches the degree of fuzzing associated with the FIA plot locations, so that fuzzing is unlikely to add substantial error in the estimation of CWD experienced at the true plot location. For each plot, we calculated the annual mean growing season (May-October) CWD estimates for 2000 to 2020. The distribution of annual mean growing season CWD estimates for each plot informed two variables: Site dryness (calculated as the mean of the annual mean values) and

drought (calculated as the 90th percentile of the annual mean values).

2.4. Analytical overview

Our analyses were guided by well-established FIA procedures (i.e., estimating changes in tree populations, Scott et al., 2005) and by recent progress in the application of FIA data to assess the impact of biological and environmental agents on tree vital rates (Shriver et al., 2021). Prior to any modeling, we inspected and summarized the inventory data from FIA. To quantify recent changes (i.e., last ten years) in sugar pine abundance across its range (i.e., Oregon and California), we calculated the annual percent change in live tree density for plots remeasured between 2010 and 2019.

While demographic modeling provides valuable insights regarding the range-wide vulnerability of trees (Ohse et al., 2023), the FIA data (e.g., Shriver et al., 2021) and the demographic modeling (e.g., Doak et al., 2021) present challenges. To navigate these challenges, we followed the workflow for building an integral projection model (IPM) outlined in Doak et al. (2021). We used data for individuals greater than 2.54 cm DBH on every plot where sugar pine was present at initial measurement or remeasurement (1221 plots). We then fit statistical models to the vital rate data extracted from FIA. Given the well-established influence of tree size on vital rates (Needham et al., 2018), we modeled survival, growth, and recruitment as continuous functions of tree size. We generated covariates based on the presence or severity of known stressors and included them as continuous state variables in our survival and growth functions. Next, we built a structured population model from these vital rates. We combined the vital rate functions into projection kernels to forecast decadal trends in sugar pine abundance. We integrated each projection kernel across 99 size classes and analyzed the results to estimate the asymptotic population growth for sugar pine under various scenarios. Throughout, we relied on advice distilled from recent comments in the literature to guide how we built and tested our structured population model (Doak et al., 2021; Merow et al., 2014). For example (more details below), we constructed the size bins in such a way as to avoid the problem of evicting overlarge individuals from the IPM and used the cumulative density function difference method to discretize the continuous growth kernel when constructing the IPM.

2.5. Changes in abundance

The FIA growth, removals, and mortality (GRM) estimator provides a robust, annual estimate of population change by combining Phase 2 inventory data (on-the-ground sampling) with strata defined by Phase 1 sampling (remotely sensed classification of the landscape; Scott et al., 2005). For our population of interest, namely sugar pine trees in California and Oregon, we used the rFIA package (Stanke et al., 2020). The mean annual percent change in density was calculated for trees $\geq$12.7 cm with 95% confidence intervals based on a t-distribution.

2.6. Vital rates models

As noted by Shriver et al. (2021), a weakness in the FIA data for demographic analysis is that the fates of individual seedlings (stems <2.54 cm DBH) are not tracked between inventories. The inventories include only counts of live seedlings. Shriver et al. (2021) demonstrated an effective solution that leveraged the seedlings counts and relied on jointly modeling survival, growth, and fecundity to estimate recruitment. However, this approach when applied to our sugar pine analysis performed poorly. A minor overestimation of the growth rate for the smallest stems resulted in a major overestimation of the recruitment rate. Instead, we limited the definition of recruits to tagged trees growing into the smallest size class (stems $\geq$ 2.54 cm DBH) since the last inventory and modeled vital rates independently using the observed data. However, our vital rate models did follow the functional forms used in Shriver et al. (2021).

The model for survival is:

$$s_i \sim \text{Bernoulli}(p_i) \tag{1}$$

$$\text{logit}(p_i) = \mathbf{X}_{i,*}\beta_{(s)} + \gamma_{(s)j} + \delta_{(s)k} \tag{2}$$

where s_i is an integer indicating the live/dead status (1 if live, 0 if dead) of individual i at the revisit measurement (approximately 10 years after initial measurement), p_i is the probability of survival from initial measurement to remeasurement, $\mathbf{X}_{i,*}$ is a row vector of covariates (described below) for individual i, $\beta_{(s)}$ is a column vector of fixed effect coefficients for the survival sub model, $\gamma_{(s)}$ is a vector of plot-level random effects indexed by the plot j for individual i with $\gamma_{(s)j} \sim \text{N}(0, \sigma^2_{\gamma(s)})$, and $\delta_{(s)}$ is a vector of ecoregion subsection-level random effects indexed by the ecoregion subsection k for individual i with $\delta_{(s)k} \sim \text{N}(0, \sigma^2_{\delta(s)})$. Plot and ecoregion random effects were included to ensure independence of residuals in a context where there are potentially unmeasured covariates affecting vital rates at fine spatial scales (plot level random effects) or coarse spatial scales (ecoregion level random effects).

The model for growth is:

$$z_i \sim \text{Normal}\left(\mu_i, \sigma^2_\varepsilon\right)\text{T}[0.0254,] \tag{3}$$

$$\mu_i = \mathbf{X}_{i,*}\beta_{(z)} + \gamma_{(z)j} + \delta_{(z)k} \tag{4}$$

where z_i is the DBH in meters of individual i at remeasurement drawn from a truncated normal distribution (to prevent excluded-by-sampling-design size below 2.54 cm DBH), μ_i is the mean predicted DBH of individual i at remeasurement, σ^2_ε is the residual variance, $\mathbf{X}_{i,*}$ is a row vector of the fixed effects covariates, and the other parameters are as defined for the survival sub model, though here indexed z to indicate that they are the parameters specifically for the growth sub model. The fixed effect covariates for the growth model are the same as those for the survival model. Note that the coefficient for the main effect of initial size should be very close to 1, because the size at remeasurement is primarily determined by the initial size.

The response distribution for the fecundity model is:

$$\text{c}'_j \sim \text{Neg.Binomial}(\mathbf{n}'_j \times a, \kappa) \tag{5}$$

where c'_j is the observed count of new recruits (individuals between 2.54 cm and 12.7 cm DBH which were newly present at the follow up census) on plot j. $\mathbf{n}'_j$ is the area-standardized occurrence rate of new recruits on plot j at remeasurement, a gives the total plot area surveyed for individuals between 2.54 cm and 12.7 cm DBH, and κ is the dispersion parameter for the negative binomial distribution.

The area-standardized occurrence rate of new recruits ($\mathbf{n}'_j$) is the sum of the fecundity of each of 99 size classes (2.54 to 250.4 cm DBH in 2.54 cm wide bins):

$$\mathbf{n}'_j = \sum_{k=1}^{99} f \times \mathbf{n}_{j,k} \tag{6}$$

where f is the fecundity (the number of new recruits produced per existing individual) and $\mathbf{n}_{j,k}$ is the area-standardized occurrence rate of individuals in the kth size class at the initial census. The low frequencies of new recruits in the data (942 of the 967 observed plots had no new recruits) precluded estimation of a more complex fecundity function which would have allowed fecundity rates to vary by individual sizes and/or the presence of stressors, as with the survival and growth functions. Instead, we estimated a simple overall fecundity rate using an intercept-only linear model with a log link:

$$\log f = \beta_{0(f)} \tag{7}$$

where $\beta_{0(f)}$ is the intercept for the log-scale linear predictor of fecundity.

We developed two sets of vital rate models, the first intended to

assess overall population trajectories within each ecoregion and the second to understand which stressors are having the largest impact on vital rates. The two sets of vital rate models are distinguished by the which covariates are included in the row vector $\mathbf{X}_{i,*}$ for each individual i of a given size. In the first (population assessment) set of vital rates, the fixed effects are: The intercept (*INTERCEPT*), the DBH in meters at initial measurement (*DBH*), and the squared DBH (DBH^2). A quadratic effect of size was included to allow the vital rate functions to capture potentially nonlinear relationships between size and vital rates (e.g. allowing growth expressed as diameter increment to be low for saplings, high for midsize trees, and decline for the largest trees). Only size and random effects (both plot and ecoregion) were included in the first suite of vital rate models so that the fixed effects (for the intercept, size, and quadratic size) reflect aggregate conditions across all plots regardless of whether they were exposed to potential stressors (e.g., fire, drought, or WPBR).

For the second set of vital rate models, we included additional covariates representing the major stressors facing sugar pine. We defined major stressors as those likely to impact sugar pine persistence. However, given the dependencies among morality agents, attribution of losses poses challenges (Das et al., 2016). The most important challenge was separating losses due to fire and drought from losses due to timber harvest. FIA assessments identify trees that were lost due to cutting. These intentional removals are assumed to be used and reported as timber harvest. For sugar pine trees ($\geq$ 12.7 cm DBH), the loss rate due to these harvests was 0.64% yr^{-1} (2010–2019) which accounts for 25% of all sugar pine deaths (Data: FIA Phase 2 Database version 1.8.0.03). From this perspective, harvest is clearly a major stressor. However, some of the cutting was part of post-fire salvage operations or hazard tree removals. In other words, not all the cut trees were part of a planned silvicultural operation, but rather were emergency responses to fire and drought-induced deaths. For example, 12.5% of the plots with cut trees had the presence of fire recorded in the disturbance codes (DSTRBCD in the FIA database). In addition, during the remeasurement interval there was mass tree mortality related to the 2012–2016 hotter drought with losses concentrated in the heart of sugar pine's range (Stevens et al., 2017; Stephenson et al., 2019). In response to the risks posed by such widespread mortality, a joint federal and state task force removed more than 1.6 million dead "hazard" trees in California (California Wildfire and Forest Resilience Task Force, 2023). Given these dependencies, we choose not to exclude cut trees from our analysis so not to underestimate the impacts of fire and drought, and to get a realistic understanding of the population trajectory in contexts where other stressors are absent. Therefore, we included cut trees in our reference scenario (see explanation below). We note that our findings are robust to this inclusion of harvested plots: When we excluded plots with harvested sugar pines and re-ran the entire analysis (described below), the results were virtually identical to those presented in this manuscript (Supplementary Figure 3). Insect attacks, especially bark beetle outbreaks induced by drought (*sensu* Fettig et al., 2019), can also be an important mortality agent. However, only rarely (2.5% of plots) were bark beetles reported as a disturbance. Thus, we included four major stressors as covariates in our vital rate models: fire, WPBR, competition, and water stress.

We modeled these major stressors as fixed effects covariates represented by the row vector $\mathbf{X}_{i,*}$. Specifically, the fixed effects are: The intercept (*INTERCEPT*), the DBH in meters at initial measurement (*DBH*), the squared DBH (DBH^2), a binary flag indicating whether the individual's plot experienced a fire at least 0.404 ha in size that killed or damaged at least 25% of trees between initial measurement and remeasurement (*FIRE*), a binary flag indicating whether any trees in the individual's plot displayed signs of white pine blister rust infection at initial measurement (*WPBR*), the plot-level live basal area (BA) at initial measurement (*BA*; a proxy for competition, Eitzel et al., 2013), the plot-level 90th percentile of growing season departure from mean climatic water deficit (*DROUGHT*) between initial measurement and remeasurement, the plot-level growing season mean climatic water deficit over the period 2000–2020 (*DRYNESS*), and interactions between *DBH* and DBH^2 and all other variables ($DBH \times FIRE$, $DBH^2 \times FIRE$, $DBH \times WPBR$, $DBH^2 \times WPBR$, $DBH \times BA$, $DBH^2 \times BA$, $DBH \times DROUGHT$, $DBH^2 \times DROUGHT$, $DBH \times DRYNESS$, and $DBH^2 \times DRYNESS$). We included size (and quadratic size) and added the interactions between size (and quadratic size) and the stressors given that the impacts of these stressors are size-contingent (Hood et al., 2007; Stephenson et al., 2019; Dudney et al., 2020). *BA*, *DROUGHT*, and *DRYNESS* were centered and scaled to have 0 mean and unit variance across all plots. We used size on the meter scale so that size was on a similar scale as the other explanatory variables, which improved the model's performance during parameter estimation (details below).

Model data were prepared using the tidyverse package (Wickham et al., 2019) in R Version 4.1.1 (R Core Team, 2021), and Bayesian parameter estimation was performed using Hamiltonion Monte Carlo as implemented in Stan version 2.28.2 (Stan Development Team, 2022). The sampler was run in four chains for 2000 iterations per chain (discarding the first 1000 iterations as warmup). The prior distribution specified for all parameters was Normal$(0, 5)$ (with variance terms restricted to positive values) except for the negative binomial dispersion parameter κ, which received a Cauchy$(0, 5)$ prior following Shriver et al. (2021). Other R packages used for data preparation, statistical analysis, and processing of results were bayesplot (Gabry and Mahr, 2021), cmdstanr (Gabry et al., 2022), cowplot (Wilke, 2020), DBI (R-SIG-DB et al., 2021), ggspatial (Dunnington, 2021), here (Müller, 2020), posterior (Bürkner et al., 2021), raster (Hijmans, 2021), RSQLite (Müller et al., 2021), sf (Pebesma, 2018), spData (Bivand et al., 2021), tmap (Tennekes, 2018), units (Pebesma et al., 2016), and USAboundaries (Mullen and Bratt, 2018).

2.7. Model checking

The basic diagnostics provided by cmdstanr (R-hat values, effective sample size, trace plots, per-chain posterior density plots, posterior pair plots, and assessment of divergences) were inspected for evidence of convergence and between-chain consistency or signs of difficulty estimating parameters. To assess the out-of-sample predictive performance of the models, 10% of plots were randomly held out of the training dataset used to estimate parameters. For both the training and validation data sets, the central tendency and spread of data simulated using posterior parameter values (posterior predictions) were compared to the true observed values of individual growth and individual survival to assess whether model results were consistent with empirical results. Likewise, we compared histograms of observed vs. simulated counts using the estimated fecundity rate to assess whether model results were consistent with real data.

2.8. Evaluation of vital rate functions

Once parameters were estimated and model validity checked, the fitted model for vital rate functions was used to assess the impact of size and the various stressors (fire, WPBR, competition, and water stress) on the vital rates of growth and survival. Effect strength was assessed in relative terms based on the magnitude of the median parameter estimate and the coverage of the 90% quantile-based credible interval (CI). For the survival model, fixed effects coefficients whose median absolute value exceeded 2.0 (on the logit scale) were interpreted as strong, while effects whose median absolute value was less than 2.0 but whose CI excluded 0 were interpreted as moderate. For the growth model, fixed effects coefficients whose CI excluded 0 were interpreted as significant. For both models, the effect of a stressor on a vital rate was interpreted as weak or uncertain if the CI for the associated fixed effect included 0. The choice of 90% quantile-based credible intervals follows the conventions of the posterior package in R (Bürkner et al., 2021), though any specific threshold for significance is somewhat arbitrary (McElreath, 2016).

To provide more nuanced insight into the effects of the various stressors than simple hypothesis tests, we constructed posterior predictions to represent a suite of hypothetical environmental scenarios designed to evaluate the effect of a single stressor. The reference scenario serves as a null model where the major stressors are absent (i.e., *FIRE* and *WPBR*) or held at their mean value (i.e., *BA*, *DROUGHT*, and *DRYNESS*). As noted above, the reference scenario for survival includes cut trees. The remaining scenarios correspond to situations where a single stressor is present (in the case of the discrete explanatory variables *FIRE* and *WPBR*) or elevated/depressed by one standard deviation (in the case of the continuous variables *BA*, *DROUGHT*, and *DRYNESS*), while other stressors are absent or held at their mean value (0 for scaled variables). Given these environmental contexts, vital rates for individuals ranging in size from 0.0254–1.25 m DBH (up to approximately the 95th percentile individual size observed) were predicted using the parameters from each posterior sample, and the predicted response plotted against DBH and stressor.

2.9. Construction of IPM models

To assess the population trajectories within each ecoregion in sugar pine's range, and to understand the demographic implications of the stressors' impacts on vital rates, we constructed two suites of integral projection models (Merow et al., 2014; Needham et al., 2018; Doak et al., 2021).

In the first suite of IPMs, intended to assess the population trajectories of sugar pine across its range, we constructed an integral projection model transition kernel for each ecoregion c and posterior draw d. Each transition model kernel $\mathbf{A}_{c,d,*,*}$ is a 99×99 discretized integral projection model kernel describing the rates of transition from each $v = 1, 2, \ldots, 99$ size classes (each 2.54 cm DBH wide) into $u = 1, 2, \ldots, 99$ size classes over the course of a single 10-year census interval. The largest individual appearing in the vital rates datasets was 2.45 m DBH, though even larger sugar pines have been recorded. The elements of this matrix are a function of the parameters for the survival, growth, and fecundity functions and the data describing scenario-specific covariates, as described below. A separate $\mathbf{A}_{c,d,*,*}$ exists for each ecoregion c and posterior draw d. The elements of $\mathbf{A}_{c,d,*,*}$ for each ecoregion c and draw d are given by:

$$\mathbf{A}_{c,d,u,v} = p_{c,d,v} \bullet g_{c,d,u,v} + r_u \bullet f_d \tag{8}$$

where $p_{c,d,v}$ is the proportion of individuals in size class v which will survive the 10-year census interval for ecoregion c using the dth draw of the survival parameters, $g_{c,d,u,v}$ is the proportion of surviving individuals in class v which grow into class u during the census interval for ecoregion c using the dth draw of growth parameters, r_u is the probability that a new recruit will transition into size class u by the end of the 10-year interval, and f_d is the number of new recruits generated per existing individual using draw d of the fecundity parameters.

Following the recommendations of Doak et al. (2021), the continuous growth kernel described in Eq. 3 is discretized into size class transition probabilities using the cumulative density function difference method. That is, $g_{c,d,u,v}$ is the probability that an individual in ecoregion c with DBH equal to the midpoint of size class v will have a DBH at remeasurement somewhere between the upper and lower bounds of size class u, and is given by:

$$g_{d,j,u,v} = \frac{\Phi\left(\text{Upper}_u | \mu_{c,d,v}, \sigma^2_{\varepsilon,d}\right) - \Phi\left(\text{Lower}_u | \mu_{c,d,v}, \sigma^2_{\varepsilon,d}\right)}{1 - \Phi\left(0.0254 | \mu_{c,d,v}, \sigma^2_{\varepsilon,d}\right)} \tag{9}$$

where Φ is the cumulative probability density function of a normal distribution with mean $\mu_{c,d,v}$ and variance $\sigma^2_{\varepsilon,d}$ evaluated at three locations: 1) The upper bound of size class u (Upper_u), 2) the lower bound of size class u (Lower_u), or 3) at 0.0254 m (the minimum modeled size). This is an exact method for calculating the area under the probability density function for the growth kernel. This area is then normalized by that portion of the kernel in the modeled size range. $\mu_{c,d,v}$ is calculated for each draw d, ecoregion c, and size class v from Eq. 4 using the midpoint DBH of size class v and the random intercept for ecoregion c. We included a plot random effect when estimating the vital rate parameters so that the estimates for fixed effects and ecoregion random effects properly reflect the plot-level correlations among many of the observed individuals. However, because this analysis was focused on macro-scale trends, the fine-scale plot random effects were assumed to sum to 0 within each ecoregion and were not included when calculating the elements of the transition matrices.

Likewise, $p_{c,d,v}$ is calculated using Eq. 2 to predict the proportion of those individuals whose DBH is equal to the midpoint of size class v in ecoregion c which survive to the second census (using parameter values from draw d). We used the observed size distribution of new recruits to calculate the proportion of new recruits falling into each 2.54 cm bin, giving $r_u \cong [0.72, 0.10, 0.10, 0.08, 0, \ldots, 0]$. Eviction from the largest size class is avoided by setting an extremely high upper size bound for the largest class, such that portion of individuals growing beyond the maximum bound is numerically indistinguishable from 0.

We estimated asymptotic population growth rate of sugar pine within each ecoregion using this suite of IPM transition kernels. The largest real eigenvalue of each full transition matrix corresponds to the asymptotic population growth rate $\lambda_{c,d}$ for ecoregion c and posterior draw d. The distribution across draws of $\lambda_{c,*}$ for each ecoregion c was mapped to assess the overall population trajectory (including parameter uncertainty) in each ecoregion.

The second suite of IPMs was constructed to understand how the various stressors impact the demographic outlook for sugar pine. In this second suite, we constructed an integral projection model transition kernel for each hypothetical environmental scenario e (described above) and posterior draw d, simply replacing c with e in the above description of the IPM construction (Eqs. 8 and 9). Vital rates for each scenario were projected using the vital rate functions which incorporate the presence/strength of stressors at the plot level. Because the objective was to better understand the influence of the stressors on vital rates (i.e., the fixed effects), the calculation assumes that both the plot random effect and the ecoregion random effect are equal to 0. The distribution of $\lambda_{e,*}$ for each scenario e was plotted to understand how the presence or absence of different stressors is expected to shape the asymptotic population growth rate. In each scenario, each posterior sample of the parameters is used to calculate a transition matrix for a population of sugar pines on an idealized plot where the fixed effect covariates (other than size) for the vital rate models are held to specific values representing each scenario. For each of the nine scenarios, one transition matrix is constructed using the parameter values from each of the 4000 posterior draws. The dominant eigenvalue of each matrix gives the estimate of λ for that scenario and draw.

We also used the constructed transition kernels for the hypothetical environmental scenarios to project the sugar pine abundance over the course of a single census interval (i.e., 10 years):

$$\mathbf{n}'_{c,d,*} = \mathbf{A}_{c,d,*,*} \times \mathbf{n}_* \tag{10}$$

where $\mathbf{n}'_{c,d,*}$ is the 99×1 vector giving the projected stem density of individuals in each of the 99 size classes for scenario c and draw d, $\mathbf{A}_{c,d,*,*}$ is the transition kernel for scenario c and draw d, and $\mathbf{n}_*$ is the 99×1 vector giving the mean (across all real plots) stem densities of individuals in each of the 99 size classes. These projected size distributions were summed to get a total stem density projection for each scenario c and draw d to better understand how the various stressors contributed to the observed trends in abundance on the FIA plots. To evaluate trends, we compared the projected stem densities against the mean observed density from the 2000–2009 census interval (Supplementary Figure 4).

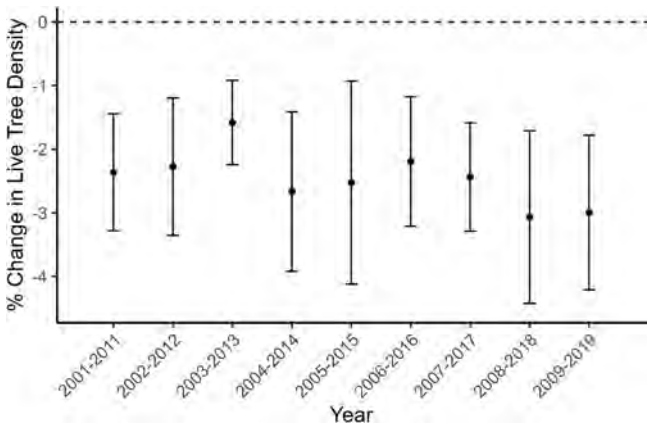

Fig. 2. Annual percent change in sugar pine live tree density for 10-yr panels from 2001–2019 for California and Oregon. Error bars represent 95% confidence intervals. Dotted line represents no change (0% change). Results include stems greater than or equal to 12.7 cm DBH.

3. Results

3.1. Changes in abundance

The abundance of sugar pine consistently declined between 2011 and 2019 (Fig. 2). Annual percent change in live tree density ranged from –3.1% yr^{-1} (2008–2018) to –1.6% yr^{-1} 2003–2013) with a median decline of –2.4% yr^{-1}. The absolute change in live tree density for trees ≥12.7 cm between 2010 and 2019 was –8% with mean range-wide density (±standard deviation) declining from 2.8 (0.1) to 2.5 (0.1) trees ha^{-1} (Supplementary Figure 5a). Trends in basal area were also negative but the drop was not as step. Basal area declined by 2.8% in the interval from 0.48 (0.02) to 0.46 (0.02) m^2 ha^{-1} (Supplementary Figure 5b).

3.2. Model checking

Diagnostics for mixing, convergence, R-hat, and transitions all indicated that the model fitting algorithm performed well. Comparisons of posterior distributions with prior distributions showed that the posterior was strongly informed by the data, rather than the prior, for most parameters (Supplementary Figures 6–11). The exceptions, where the posterior was only weakly informed by the data, were the estimates for the interactions of WPBR with size and quadratic size affecting survival. This uncertainty regarding interactions involving WPBR was likely due to the relatively low frequency of WPBR presence in the data. Posterior predictions generated using the posterior parameter samples and the training data as explanatory variables were consistent with the true values observed in the training data, with the true values nearly always falling within the range of variation predicted by the model (Supplementary Figure 12, Supplementary Figure 13, and Supplementary Figure 14). The survival model appeared slightly underconfident, in that true survival rates were slightly lower than predicted survival rates for $p_s < 0.8$, and true survival rates were slightly higher than predicted survival rates for $p_s > 0.8$. The growth model performed well, with a strong linear relationship between mean predicted and observed individual size at remeasurement. The frequency distribution of simulated new recruit counts closely matched the observed frequency distribution of recruit counts. Simulations generated using the posterior parameter and the held-out validation data as explanatory variables (survival: Supplementary Figure 16, growth: Supplementary Figure 16, and fecundity: Supplementary Figure 17) were broadly consistent with the true values observed in the validation data.

3.3. Survival

There was a strong positive effect of size on survival, with a negative quadratic effect (Table 1). Median posterior predicted 10-year survival rates increased from approximately 84% for stems with 0.0254 m DBH up to a maximum of 96.5% for stems with 0.88 m DBH, before falling off for the largest stems (Fig. 3a). Of the 171 individuals with DBH >1.25 m at the initial census, only 135 (78.9%) survived to the remeasurement. However, there was large uncertainty about survival rates for the largest stems because there were few extremely large individuals. There was a strong negative main effect of fire, a positive interaction between fire and size, and a negative interaction between fire and squared size. These results indicate that fire substantially reduced survival, particularly for the smallest and largest trees (Fig. 3b). There were moderate negative effects of WPBR and basal area on survival (Fig. 3c and d). Other effects were weak or uncertain (their 90% quantile-based credible intervals overlapped 0; Fig. 3e and f).

3.4. Growth

The effect of initial tree size on growth followed a quadratic function

Table 1
Summary of results for survival sub model, giving (from left to right) the mean, median, standard deviation, 5th percentile, and 95th percentile of posterior samples for each parameter, plus diagnostics R-hat, effective sample size (bulk), and effective sample size (tail).

Parameter	Mean	Median	StDev	q5	q95	rhat	ess_bulk	ess_tail
Intercept	1.60	1.60	0.26	1.18	2.01	1.00	1506.35	2415.77
DBH (m)	3.96	3.95	0.79	2.70	5.28	1.00	1344.03	2318.48
DBH^2 (m)	–2.26	–2.26	0.57	–3.23	–1.36	1.00	1416.84	2254.01
Fire	–4.10	–4.10	0.59	–5.11	–3.14	1.00	1546.32	2135.26
WPBR	–1.06	–1.05	0.57	–1.99	–0.15	1.00	1589.91	1892.62
Basal Area	–0.66	–0.66	0.23	–1.05	–0.28	1.00	1403.30	2244.98
Drought	–0.18	–0.18	0.21	–0.51	0.17	1.00	1417.02	2248.52
Site Dryness	–0.33	–0.32	0.23	–0.73	0.04	1.00	1398.86	1813.38
DBH x Fire	3.70	3.70	1.52	1.21	6.22	1.00	1282.09	2077.02
DBH^2 x Fire	–1.65	–1.63	0.96	–3.24	–0.10	1.00	1234.10	1951.74
DBH x WPBR	0.01	0.01	1.88	–3.08	3.14	1.00	1695.31	2146.93
DBH^2 x WPBR	0.53	0.52	1.42	–1.78	2.85	1.00	1872.47	2281.46
DBH x BA	0.74	0.74	0.56	–0.19	1.63	1.00	1512.10	2145.78
DBH^2 x BA	–0.11	–0.11	0.32	–0.63	0.44	1.00	1563.40	2360.91
DBH x Drought	–0.02	–0.03	0.61	–0.99	1.01	1.00	1413.84	2175.04
DBH^2 x Drought	0.08	0.09	0.42	–0.62	0.75	1.00	1495.65	2166.34
DBH x Dryness	0.62	0.61	0.70	–0.50	1.77	1.00	1188.31	1779.99
DBH^2 x Dryness	–0.61	–0.60	0.49	–1.42	0.20	1.00	1291.86	1850.61
SD Plots	2.00	2.00	0.16	1.75	2.27	1.00	1131.53	2272.20
SD Ecoregions	0.28	0.26	0.17	0.03	0.59	1.01	521.18	1116.88

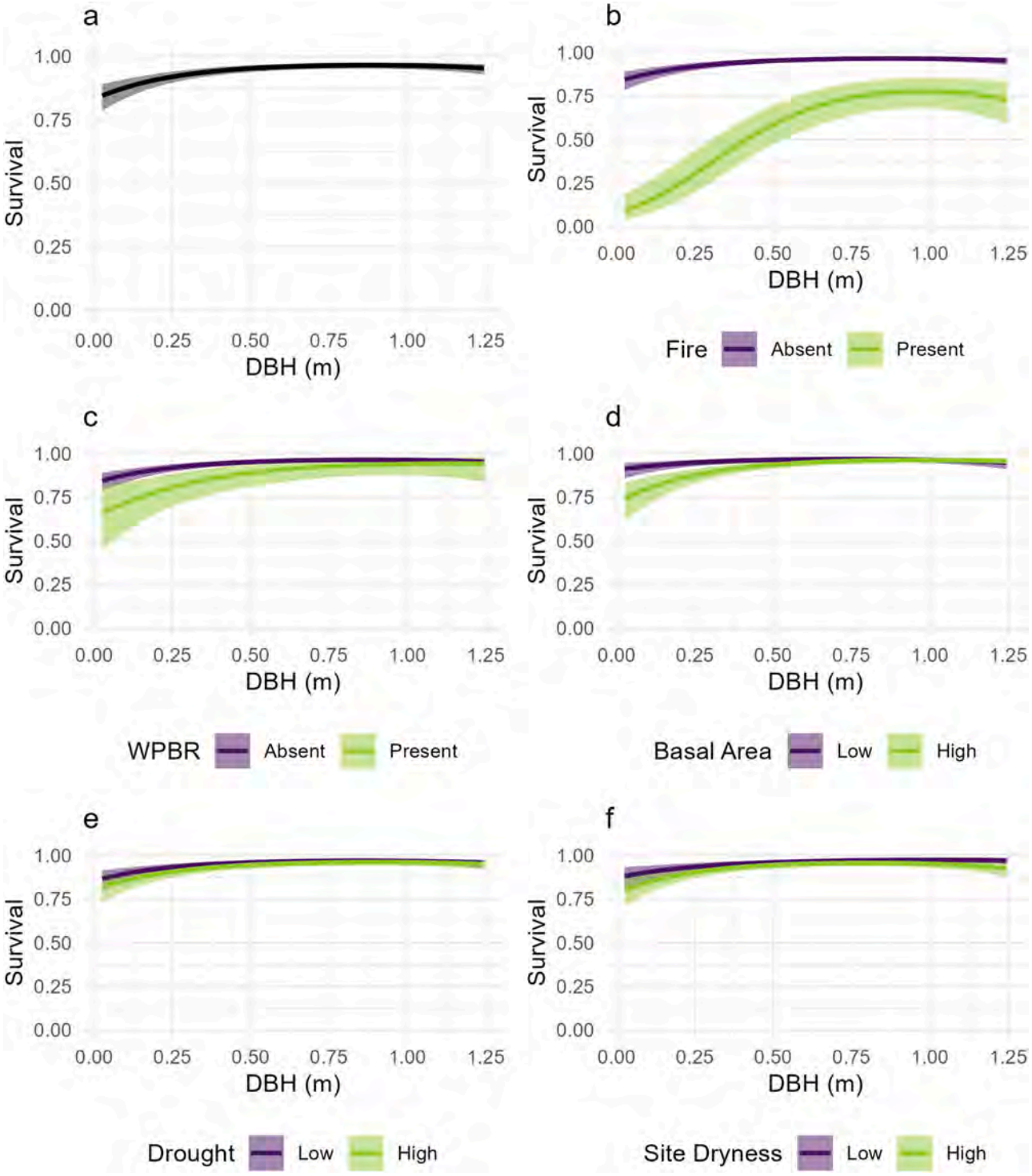

Fig. 3. Fixed effects of initial DBH, fire, WPBR, neighborhood basal area, drought, and site dryness on 10-year survival probability. In panel (a), probability of survival (Y-axis) is predicted for stems of various initial size (X-axis), holding other variables at "Absent" (for fire and WPBR) or 0 (scaled mean, for basal area, drought, and site dryness). In the other panels (b-f), probability of survival is predicted for stems of various sizes and across two levels of each other explanatory variable: with or without disturbance, or at high (1.0) or low (−1.0) values for scaled continuous variables. Predictions were generated using the posterior samples for model parameters, resulting in a range of predicted survival for each set of explanatory variable values. Lines show the median predicted survival and lighter ribbons show a 90% quantile-based credible interval. Random effects were held at 0. 1.25 m is approximately the 95th percentile DBH of trees used to train the model.

with growth peaking in the mid-size trees (Fig. 2a). The posterior median for the intercept of the model for size at the second census was 0.018, with a 90% credible interval from 0.014 to 0.022 (Table 2). The effect of initial size was, as expected, very close to 1, and the quadratic effect of initial size was negative. Together, these results indicate that the smallest and largest trees grew approximately 2.5 cm DBH in the 10 years between initial and follow-up census, with midsize trees (initial DBH approx. 0.70 m) growing faster, at around 4.4 cm in 10 years (Fig. 4a). Though all three fire effects were weak or uncertain individually (Table 2), their aggregate effect was to significantly reduce the

Table 2
Summary of results for growth sub model, giving (from left to right) the mean, median, standard deviation, 5th percentile, and 95th percentile of posterior samples for each parameter, plus diagnostics R-hat, effective sample size (bulk), and effective sample size (tail).

Parameter	Mean	Median	StDev	q5	q95	rhat	ess_bulk	ess_tail
Intercept	0.018	0.018	0.003	0.014	0.022	1.00	1932.23	2370.47
DBH (m)	1.076	1.076	0.006	1.067	1.086	1.00	3524.26	3051.14
DBH^2 (m)	–0.056	–0.056	0.004	–0.063	–0.049	1.00	3626.18	3225.29
Fire	–0.007	–0.007	0.007	–0.019	0.005	1.00	2513.11	2712.72
WPBR	0.011	0.011	0.005	0.003	0.020	1.00	2895.99	2856.91
Basal Area	–0.013	–0.013	0.002	–0.017	–0.010	1.00	4376.90	3496.19
Drought	–0.002	–0.002	0.002	–0.005	0.000	1.00	3798.53	3164.24
Site Dryness	–0.007	–0.007	0.002	–0.010	–0.003	1.00	3209.21	3237.66
DBH x Fire	–0.012	–0.012	0.018	–0.042	0.018	1.00	2332.80	2469.12
DBH^2 x Fire	0.007	0.007	0.011	–0.011	0.024	1.00	2432.29	2427.42
DBH x WPBR	–0.012	–0.012	0.016	–0.038	0.015	1.00	3008.42	2767.14
DBH^2 x WPBR	0.000	0.000	0.011	–0.018	0.018	1.00	3138.79	2684.75
DBH x BA	0.018	0.018	0.005	0.010	0.025	1.00	4579.41	3151.88
DBH^2 x BA	–0.003	–0.003	0.003	–0.008	0.001	1.00	4548.37	2823.81
DBH x Drought	0.003	0.002	0.005	–0.006	0.011	1.00	4215.27	3110.52
DBH^2 x Drought	0.002	0.002	0.004	–0.004	0.007	1.00	4124.82	3026.97
DBH x Dryness	0.024	0.024	0.006	0.015	0.034	1.00	3594.70	2575.45
DBH^2 x Dryness	–0.016	–0.016	0.004	–0.023	–0.010	1.00	3577.96	2781.10
SD Plots	0.017	0.017	0.001	0.016	0.018	1.00	1346.76	2286.28
SD Ecoregions	0.013	0.013	0.002	0.010	0.016	1.00	1164.93	2129.77
SD Residuals	0.021	0.021	0.000	0.021	0.022	1.00	2432.84	2942.95

growth rate of stems greater than approximately 0.30 m DBH (Fig. 4b; note how the 90% CIs for growth as a function of size do not overlap between the "fire present" and "fire absent" scenarios). White pine blister rust presence actually increased the growth of the smallest stems, perhaps due to cankers increasing stem diameter or WPBR mortality reducing competition for the survivors (Fig. 4c). By contrast, increased basal area reduced the growth of small stems but not large ones (Fig. 4d). Site dryness also had a negative main effect and a positive interaction with initial size, plus a negative interaction with quadratic size: For the smallest and largest stems, growth was lower on dry sites, whereas for stems between approximately 0.40 m and 1.10 m DBH, growth was higher on dry sites (Fig. 4f). Other effects were weak or uncertain (Table 2).

3.5. Fecundity

The posterior median value for the intercept of the fecundity model was –2.94, with a 90% CI from –3.32 to –2.58 (Table 3). These parameters indicate that the average number of new recruits produced per existing tree per 10 years was 0.05 (0.04–0.08).

3.6. Asymptotic population growth rates

There were stark regional differences in the asymptotic population growth rate (λ) of sugar pine populations (Fig. 5, Supplementary Table 1; both constructed using the vital rates models where *INTERCEPT*, *DBH*, and DBH^2 were the only fixed effects). The posterior median value of λ was below one in every ecoregion, and below 0.90 in several ecoregions in the southern Sierra Nevada. The 90% credible interval for λ excluded one (the model was highly confident in predicting decline) in 15 out of 65 ecoregions.

Fig. 6 shows the posterior distribution of λ predicted from IPMs built on a variety of hypothetical scenarios (produced using vital rate functions with the full suite of fixed effects). In the reference scenario, discrete stressors (fire and WPBR) were absent, while continuous stressors (basal area, drought, and site dryness) were held at zero (their scaled means). Under these circumstances, the asymptotic growth rate is near or slightly below one, with a median posterior value of λ of 0.980 and a 90% quantile-based CI from 0.954 to 1.005 (Fig. 6, Supplementary Table 2). Where fire is present, λ is strongly reduced (median 0.644, CI 0.520 to 0.788). Where WPBR is present, the posterior distribution for λ is below 1 (median 0.947, CI 0.855 to 0.995). When basal area is lower than average, the posterior distribution of λ is near or slightly above one (median 1.001, CI 0.974 to 1.029). By contrast, when basal area is higher than average the posterior distribution of λ is below one (median 0.946, CI 0.912 to 0.976) and is clearly lower than the reference scenario. For sites experiencing low amounts of drought, the median is 0.991 and the 90% CI of λ straddles one, while for sites experiencing high drought the posterior distribution of λ is below one (median 0.967, 90% CI from 0.934 to 0.997). Likewise, on particularly dry sites the posterior distribution of λ is below one (median 0.953, 90% CI from 0.918 to 0.985). Fire has the clearest effect on λ, followed by WPBR and high basal area, and then drought and site dryness. However, the posterior median value of λ is below one even in the reference scenario, suggesting that even under "unstressed" conditions the population of sugar pine may be declining.

3.7. 10-year projections

Total stem densities were projected to decline over the duration of a single census under nearly all hypothetical scenarios, the only exception being the low basal area scenario (Supplementary Figure 4). The decline was particularly severe in the fire scenario, followed by the WPBR scenario. Declines were predicted even for reference plots, with similar declines in the high basal area, high drought, and high site dryness scenarios.

4. Discussion

This study is the first range-wide assessment of stressors impacting the vital rates and population dynamics of sugar pine. It finds that the abundance of sugar pine is declining in terms of stem density and to a lesser extent in basal area (Fig. 2 and Supplementary Figure 5). This observed decline is consistent with the asymptotic population growth rates and the 10-year stem density projections, both of which project the abundance of sugar pine to decline (Fig. 5 and Supplementary Figure 4). Though predicted population declines are particularly severe in the southern Sierra Nevada, there was strong evidence for declining population in ecoregions across the range of sugar pine. Likewise, the scenario-based IPM predicts sugar pine populations to decline even in the reference scenario (Fig. 6). The scenario-based IPM analysis allows direct comparison of the influence of fire, WPBR, stand density, short-term drought, and long-term site dryness, providing valuable guidance for managers seeking to prioritize efforts to prevent further decline.

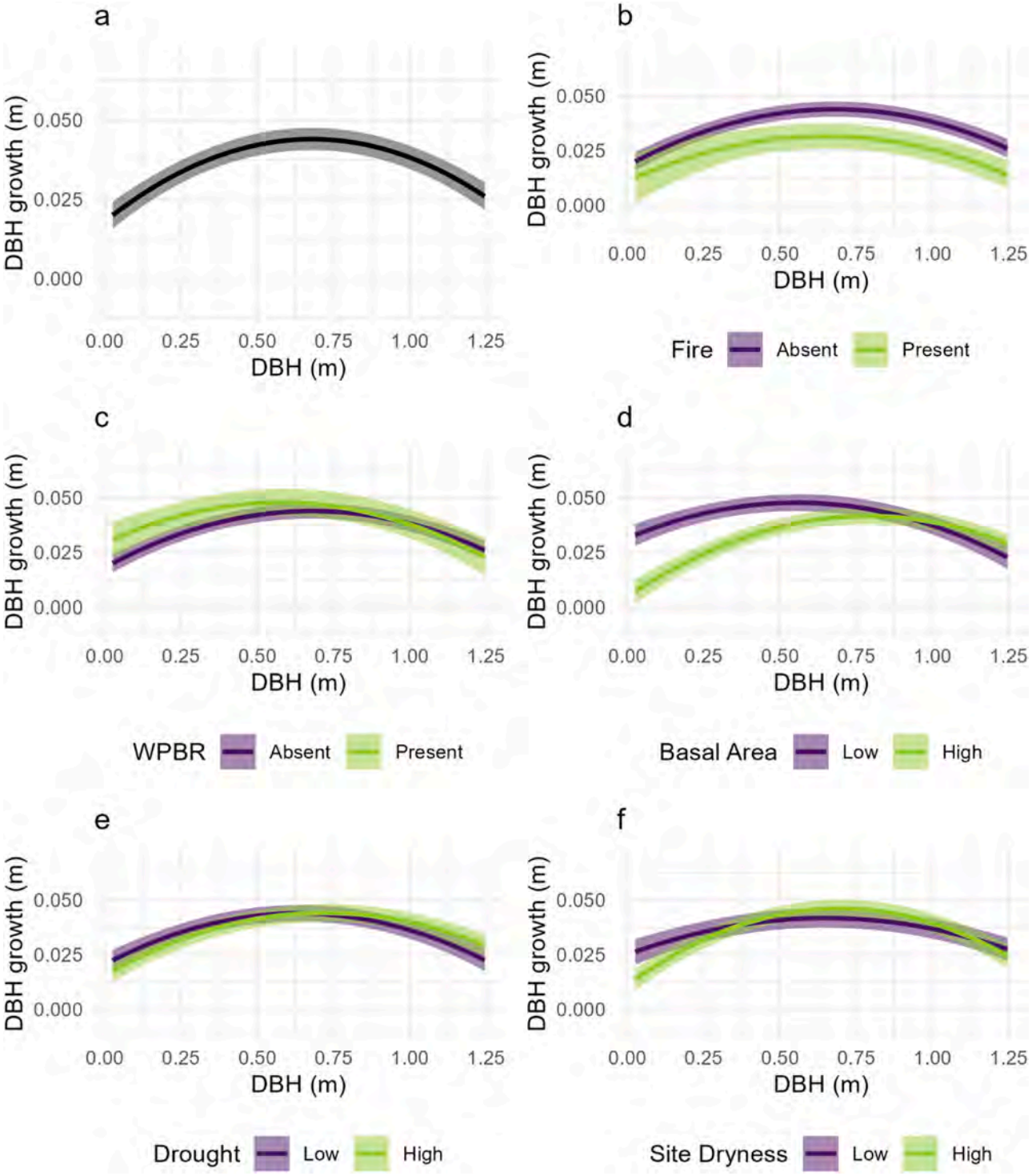

Fig. 4. Fixed effects of initial DBH, fire, WPBR, neighborhood basal area, drought, and site dryness on 10-year diameter growth. In panel (a), DBH growth over the 10 years between censuses (Y-axis) is predicted for stems of various initial size (X-axis), holding other variables at "Absent" (for fire and WPBR) or 0 (scaled mean, for basal area, drought, and site dryness). In the other panels (b-f), growth is predicted for stems of various sizes and across two levels of each other explanatory variable: with or without disturbance, or at high (1.0) or low (−1.0) values for scaled continuous variables. Predictions were generated using the posterior samples for model parameters, resulting in a range of predicted survival for each set of explanatory variable values. Lines show the median predicted survival and lighter ribbons show a 90% quantile-based credible interval. Random effects were held at 0.

The results of this study highlight fire as a key stressor negatively impacting demographic rates of sugar pine. Fire strongly reduces survival of individual trees, particularly small ones. This finding is broadly consistent with the existing literature, which has documented many cases of negative (and size-dependent) impacts of fire on the survival of sugar pine (van Mantgem et al., 2004; Hood et al., 2010; Nesmith et al., 2015; Furniss et al., 2018; Dudney et al., 2020). Fire can also injure surviving trees, reducing their growth rate as seen in this study and others (Foster et al., 2020). Reduced growth rates may have particularly strong effects on the asymptotic population growth rate in species where

Table 3
Summary of results for recruitment sub model, giving (from left to right) the mean, median, standard deviation, 5th percentile, and 95th percentile of posterior samples for each parameter, plus diagnostics R-hat, effective sample size (bulk), and effective sample size (tail).

Parameter	Mean	Median	StDev	q5	q95	rhat	ess_bulk	ess_tail
Intercept	–2.94	–2.94	0.23	–3.32	–2.58	1.00	2972.44	2109.28
NB Dispersion	0.07	0.06	0.04	0.03	0.12	1.00	2874.39	2201.71

large and old individuals disproportionately contribute to reproduction (Shriver et al., 2019); Sugar pine is one such species, though this study was unable to estimate a relationship between size and fecundity. The literature suggests that a core way in which fire influences the population dynamics of sugar pine is by killing large high-fecundity individuals (van Mantgem et al., 2004). The most extreme form of this dynamic results in type conversion, where high severity fire locally extirpates sugar pine and other mixed conifer species, resulting in the loss of mixed conifer forest generally (Shive et al., 2018; North et al., 2019; Coop et al., 2020).

In this study, the effects of fire on survival and growth combine with observed fecundity to result in posterior λ values well below one for burned plots (Fig. 6), and sharp declines in stem density projected for a single census interval (Supplementary Figure 4). However, we caution that the scenario-based asymptotic population growth rates presented in this study should not be interpreted as predictions, because in reality fire is unlikely to repeatedly occur on the same site during every census interval. Instead, the scenario-based asymptotic population growth rates give some insight into the overall influence of each stressor on population dynamics, which is supplemented by the single-step projections and the ecoregion-level projections. Existing literature has shown that most trees killed by fire die within 1 year of the fire (Furniss et al., 2018) and mortality rates in stands affected by prescribed fire returned to background levels approximately six years postfire (van Mantgem et al., 2011). These details suggest that the negative effects of fire on survival are transient. However, there is abundant evidence that the ecological footprint of fire, in particular high severity wildfire, is increasing throughout the range of sugar pine because of climate changes and biomass accumulation resulting from fire suppression (Parks and Abatzoglou, 2020; Alizadeh et al., 2021). Given this context and the results of this study, it is clear that the disrupted fire regime is a core threat facing sugar pine.

Though their effects are less severe than those of fire, both WPBR and densification negatively impact sugar pine's population dynamics in this study. The results here show that WPBR negatively impacts survival (Fig. 3). Numerous other studies have shown that blister rust tends to kill smaller trees (van Mantgem et al., 2004) and negatively affects survival rates of sugar pine and other vulnerable species (Maloney et al., 2011; Dudney et al., 2020). The presence of WPBR on individual trees (and thus on their plots) may be difficult to detect (Dudney et al., 2020), and is likely that WPBR was only detected in this study where it caused a particularly severe infection in a sampled tree. However, WPBR infections on a plot could have been missed by crews if infected trees were dead and down at the time of sampling. Given the difficulty of assessing WPBR progression as part of a decadal forest inventory, a more targeted effort is needed to better quantify the prevalence and virulence of WPBR across the range of sugar pine.

Relatively high competition (as measured by plot basal area) lowers the rates of survival for all size classes (Fig. 3). It also results in lower growth for small individuals (Fig. 4). There is extensive evidence in the literature that high neighborhood density and other proxies for competition negatively impact sugar pine survival (van Mantgem et al., 2004; Maloney et al., 2011; Levine et al., 2016) and growth (Latham and Tappeiner, 2002; Das, 2012; Eitzel et al., 2013; Steel et al., 2021). Though this study is unable to estimate how stressors affected fecundity, the literature suggests that competition may result in decreased reproduction due to stress of parent trees or decreased survival and/or growth of new recruits (Schubert, 1956; York et al., 2004, 2012; van Mantgem et al., 2006; Angell et al., 2014; Levine et al., 2016; Moran et al., 2019). In this study, high plot basal area and presence of WPBR both reduce the expected asymptotic growth rate relative to an unstressed site (i.e. reference scenario), though negative impacts are weaker than that of fire (Fig. 6, Supplementary Table 2). By contrast, reducing neighborhood basal area to one standard deviation below the mean has positive effects on λ (Fig. 6).

This study finds that long-term site dryness has clearer effects on population dynamics than does drought (i.e., departure from average climate), with site dryness having a negative impact on the growth of the largest and smallest trees. However, the asymptotic population growth rate is below one for both populations on dry sites and those experiencing drought (Supplementary Table 2). Other literature has emphasized the role of moisture stress in increased mortality rates and reduced growth among sugar pine both directly and indirectly via decreased ability of trees to resist mountain pine beetle (Das et al., 2007, 2013; van Mantgem and Stephenson, 2007; Paz-Kagan et al., 2017; Restaino et al., 2019; Bohner and Diez, 2021). However, Furniss et al. (2021) found that stand density played a more important role than climate variables in shaping mortality dynamics after fire and/or drought. Stephenson et al. (2019) examined the role of mountain pine beetle as the primary mortality agent taking advantage of widespread stress among sugar pine populations affected by drought. Intermittent droughts and/or long-term mean climatic conditions may particularly challenge small trees, causing recruitment failures even on sites where adult trees are able to persist (Bell et al., 2014; Maloney, 2014; Davis et al., 2019; Moran et al., 2019; Stewart et al., 2021). However, our analysis did not find strong effects of plot-level drought on survival. Though the extreme drought from 2012–2016 resulted in beetle epidemics that caused massive mortality among sugar pine (Stephenson et al., 2019), plot-scale drought may be a necessary but not sufficient condition for causing such epidemics: Some droughts (e.g. the 2001 drought in southern Oregon) did not resulting in widespread sugar pine mortality, but others (e.g. California's 2012–2016 drought) were associated with major mortality events.

One unexplained but troubling finding of this study is the relatively low survival rates observed for the largest sugar pines. One possible explanation is bark beetles, which are a driver of mortality for these trees: Once an outbreak is underway, beetles often preferentially kill large individuals (Stephenson et al., 2019), and localized beetle outbreaks could explain the low survival of the largest trees in these data. However, this study's finding is based on relatively few data points and should be interpreted with caution. This uncertainty regarding the outlook for the largest individuals, which are an important ecological resource (Lutz et al., 2018), highlights a need for further research.

An important limitation of this study is that it does not test for interaction between stressors in shaping vital rates of sugar pine. The complexity of the necessary models, namely three-way interactions between size and two stressors, would not only be difficult to fit given the sample size but also produce difficult-to-interpret vital rate models. Prior research suggests that a variety of such interactions may be important. For example, water stress increases the likelihood of regeneration failure, which may be a particularly acute problem in postfire landscapes where seed sources and shade trees may be limited (Davis et al., 2019; Stewart et al., 2021). A warmer and dryer climate may provide some relief from WPBR for sugar pine, as the disease's climatic envelope shifts upslope away from existing populations of sugar pine (Maloney, 2011; Dudney et al., 2021). A relationship between fire

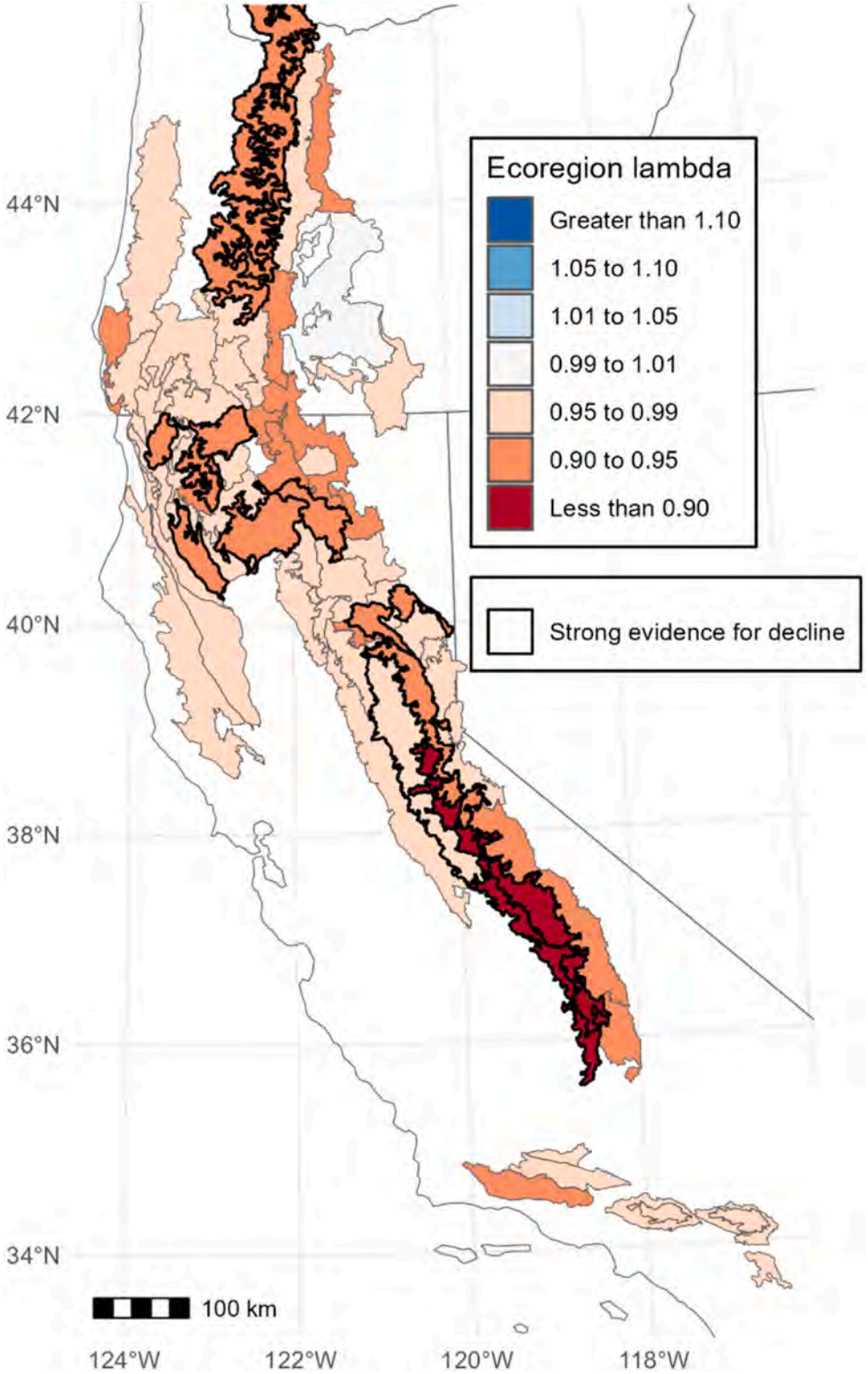

Fig. 5. Asymptotic population growth rate by ecoregion. Ecoregions are filled according to the posterior median asymptotic population growth rate from the IPM for each ecoregion. The vital rate functions for each IPM were developed using the posterior parameter values for growth and mortality as a function of size plus random-intercept ecoregion and plot effects and fecundity as an intercept only model. For the purposes of predicting ecoregion-level asymptotic growth rates, local-scale plot effects were assumed to sum to 0. Thicker black borders indicate that the 95th percentile posterior asymptotic population growth rate is below one, i.e., that there is strong evidence for population decline in the indicated ecoregion. The posterior median asymptotic population growth rate in below one in all ecoregions, and the 90% credible interval for the asymptotic population growth rate excludes one in several of them, with particularly severe population declines predicted in the southern Sierra Nevada.

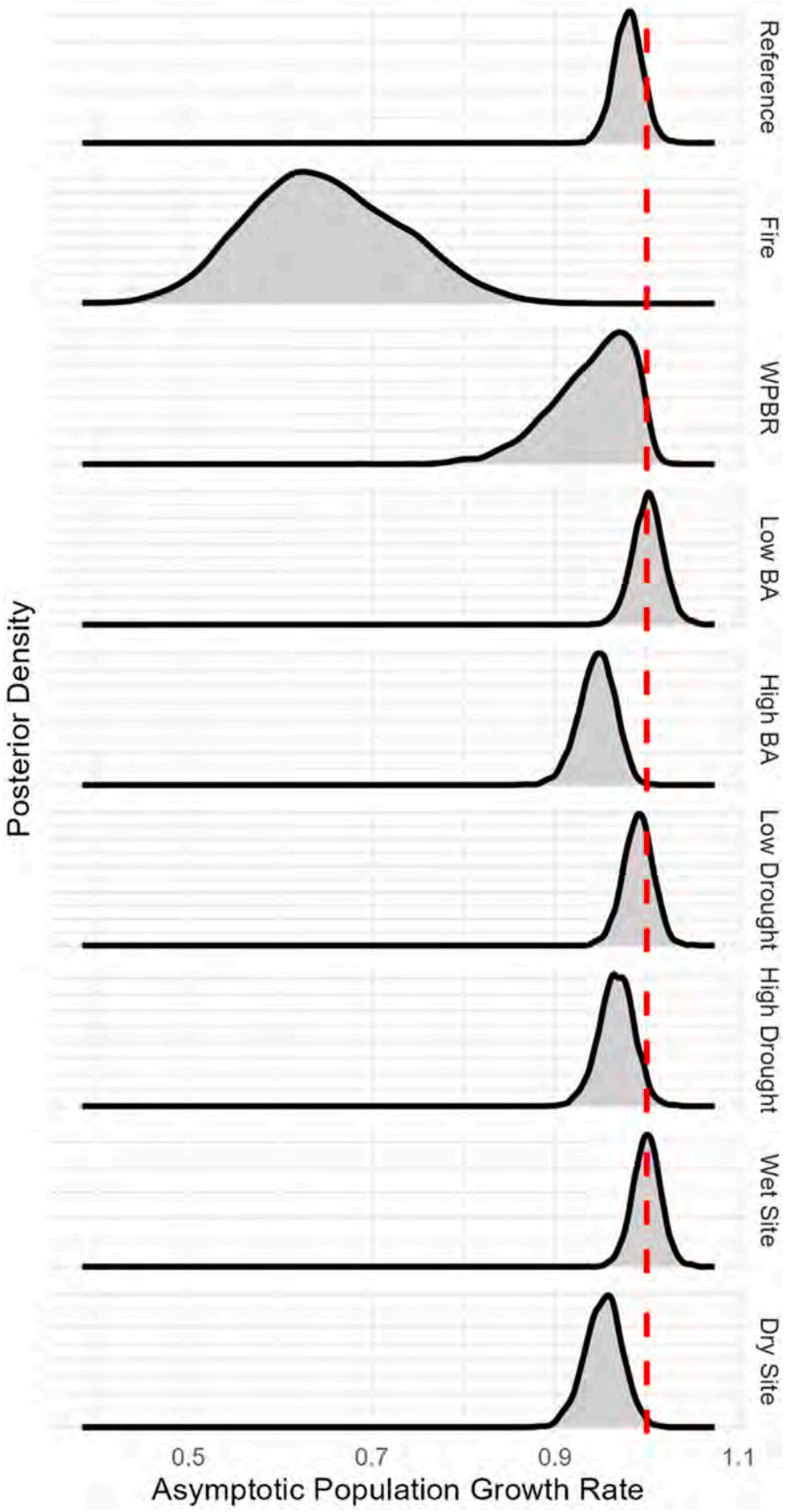

Fig. 6. Posterior distribution of asymptotic population growth rate. In the "Reference" scenario, all fixed effect covariates other than the intercept are held at 0 (representing the absence of fire and WPBR, and basal area, drought, and site dryness at average levels). In each other scenario, a single stressor is set to TRUE (for fire and WPBR), − 1 (low levels of basal area, drought, or site dryness), or + 1 (high levels of basal area, drought, or site dryness). Random effect values are held at 0, representing an average plot in an average ecoregion.

exclusion, competition, and WPBR infection has been suggested (Dudney et al., 2020), but evidence is mixed. Some studies have found that conspecific basal area was an important driver of sugar pine mortality (Das et al., 2008), but others have failed to find evidence linking fire exclusion to elevated rates of WPBR infection (van Mantgem et al., 2004; Dudney et al., 2020). Water stress and/or competition may decrease trees' ability to resist wildfire (Nesmith et al., 2015; Furniss et al., 2018, 2021; van Mantgem et al., 2018, 2020), and beetle epidemics may kill off the largest and most fire-resistant individuals (Stephenson et al., 2019; Steel et al., 2021). Water stress and densification both alter the fuel bed in ways that may increase the intensity of wildfires (Hicke et al., 2012; Stephens et al., 2018; Wayman and Safford, 2021). Likewise, wildfires may decrease trees' ability to resist bark beetles, facilitating epidemic outbreaks in the event of a post-fire drought (Davis et al., 2012; Furniss et al., 2021). Competition tends to reduce trees' ability to resist water stress and beetle epidemics (Young et al., 2017; Furniss et al., 2021; Bradford et al., 2022). Finally, there is potential for stressors to mitigate one another, primarily by a mechanism where mortality caused by one stressor results in less competitive stress and increased resilience to other stressors (van Mantgem et al., 2016; Voelker et al., 2019; North et al., 2022). For example, wildfire could reduce basal area, leaving the surviving trees better able to resist water stress over the long term. Exploring how stressors are likely to interact and shape population dynamics is another goal for future research.

5. Management implications

This study's results, which identify fire, WPBR, and competition as the major stressors of sugar pine, suggest that fuel treatments with a density reduction component could substantially benefit sugar pine populations. At first glance, this conclusion appears inconsistent with the findings of Hood et al. (2022), which found that radial thinning did not reduce the mortality rate of large sugar pines (>38 cm DBH in that study). However, close examination reveals consistency. Both this paper and Hood et al. (2022) find little-to-no effect of lower neighborhood basal area on mortality (which, in Hood et al., 2022, is driven primarily by bark beetles for large trees). Likewise, Hood et al. (2022) found that extended radius thinning increased growth of surviving trees, which is consistent with our findings that lower neighborhood basal area increases diameter growth rate for most sugar pines. Furthermore, Hood et al. (2022) report that radial thinning with a large radius increased the number of sugar pine seedlings, appearing to boost the recruitment rate. Thus, both papers are consistent in that reduced basal area have a positive effect on sugar pine population dynamics and that this effect is due to increased growth and fecundity rather than reduced mortality.

Fuel treatments to reduce or rearrange the dead biomass which fuels wildfires have been proven to reduce the hazard of severe wildfire (Stephens and Moghaddas, 2005; Stephens et al., 2009; Foster et al., 2020), and in many cases have the co-benefit of reducing basal area (Hessburg et al., 2016; North et al., 2021). Our findings, along with results from other studies examining the effects of prescribed fire on sugar pine mortality (van Mantgem et al., 2004; Steel et al., 2021a), suggest that managers should be careful in their application of prescribed fire to reduce wildfire hazard and consider measures such as raking or local density reduction to protect individual trees where pre-fire fuels are abundant (Nesmith et al., 2010; Furniss et al., 2021). Mechanical fuel treatments will provide some protection from wildfire and can be applied in combination with timber harvests, for a dual benefit of reducing wildfire hazard and competition (Collins et al., 2014; McCauley et al., 2022; Restaino et al., 2019). Managers can take advantage of established programs producing WPBR-resistant seedlings in reforestation efforts aimed at restoring sugar pine on landscapes impacted by high severity fire (Kinloch et al., 2018). Investments in artificial regeneration should likewise be made deliberately and secured with follow up treatments for wildfire hazard (North et al., 2019) and pruning to limit the effects of WPBR (Bronson et al., 2018).

Finally, contemporary timber harvest of sugar pine in California (approximately 106 million board feet per year, Marcille et al., 2020; Morgan et al., 2012) is about a third of the peak rates in the late 1980 s of over 300 million board feet per year (Western Wood Products Association, 1993). Because it was impossible to disentangle harvest as a cause of mortality and post-mortality harvests in the FIA data, this study was unable to quantify the impact of these harvest activities on the population dynamics of sugar pine. However, this study did find that even in the "reference" scenario, where most stressors other than harvests are absent, the sugar pine population is declining (λ below one). Further limiting the harvest of healthy live sugar pines is an obvious conservation strategy and should be considered when designing management plans to benefit this iconic species.

Funding

Funding for this work was provided by the United States Department of the Interior National Park Service Award #P19AC02149.

CRediT authorship contribution statement

Foster Daniel E.: Conceptualization, Data curation, Formal analysis, Investigation, Methodology, Software, Validation, Visualization, Writing – original draft, Writing – review & editing. **Stephens Scott:** Supervision, Writing – review & editing. **de Valpine Perry:** Formal analysis, Methodology, Supervision, Writing – review & editing. **Battles John:** Conceptualization, Formal analysis, Funding acquisition, Investigation, Methodology, Project administration, Software, Supervision, Visualization, Writing – review & editing.

Declaration of Competing Interest

The authors declare that they have no known competing financial interests or personal relationships that could have appeared to influence the work reported in this paper.

Data Availability

Data will be made available on request.

Appendix A. Supporting information

Supplementary data associated with this article can be found in the online version at doi:10.1016/j.foreco.2023.121659.

References

Abatzoglou, J.T., Dobrowski, S.Z., Parks, S.A., Hegewisch, K.C., 2018. TerraClimate, a high-resolution global dataset of monthly climate and climatic water balance from 1958-2015 (Available at:). Sci. Data 5, 1–12. https://doi.org/10.1038/sdata.2017.191.

Aitken, S.N., Whitlock, M.C., 2013. Assisted gene flow to facilitate local adaptation to climate change (Available at:). Annu. Rev. Ecol., Evol., Syst. 44, 367–388. https://doi.org/10.1146/annurev-ecolsys-110512-135747.

Alizadeh, M.R., Abatzoglou, J.T., Luce, C.H., Adamowski, J.F., Farid, A., Sadegh, M., 2021. Warming enabled upslope advance in western US forest fires (Available at:). Proc. Natl. Acad. Sci. 118 (22), e2009717118. https://doi.org/10.1073/pnas.2009717118.

Angell, N., Waring, K.M., Graves, T.A., 2014. Predicting height growth of sugar pine regeneration using stand and individual tree characteristics (Available at:). Forestry 87 (1), 85–97. https://doi.org/10.1093/forestry/cpt028.

Ansley, J.-A.S., Battles, J.J., 1998. Forest composition, structure, and change in an old-growth mixed conifer forest in the Northern Sierra Nevada. J. Torre Bot. Soc. 125 (4), 297–308. ⟨http://www.jstor.org/stable/29972⟩.

Bailey, R.G., 2016. Bailey's ecoregions and subregions of the United States, Puerto Rico, and the U.S. Virgin Islands. Forest Service Research Data Archive,, Fort Collins, CO. https://doi.org/10.2737/RDS-2016-0003.

Bell, D.M., Bradford, J.B., Lauenroth, W.K., 2014. Early indicators of change: divergent climate envelopes between tree life stages imply range shifts in the western United States (Available at:). Glob. Ecol. Biogeogr. 23 (2), 168–180. https://doi.org/10.1111/geb.12109.

BGCI, 2021. State of the World's Trees. Botanic Gardens Conservation International,, Richmond, UK. ⟨https://www.bgci.org/resources/bgci-tools-and-resources/state-of-the-worlds-trees/⟩. accessed 7/28/2023.

Bivand, R.S., Nowosad, J. and Lovelace, R. (2021) spData: Datasets for Spatial Analysis'. Available at: ⟨https://cran.r-project.org/package=spData⟩.

Bohlman, G.N., Safford, H.D., Skinner, C.N., 2021. Natural range of variation for yellow pine and mixed-conifer forests in northwestern California and southwestern Oregon. Gen. Tech. Rep. PSW-GTR-273. Albany, CA: US Dep. Agric., For. Serv., Pac. Southwest Res. Station 273 (November), 146.

Bohner, T., Diez, J., 2021. Tree resistance and recovery from drought mediated by multiple abiotic and biotic processes across a large geographic gradient (Available at:). Sci. Total Environ. 789, 147744. https://doi.org/10.1016/j.scitotenv.2021.147744.

Bradford, J.B., Shriver, R.K., Robles, M.D., McCauley, L.A., Woolley, T.J., Andrews, C.A., Crimmins, M., Bell, D.M., 2022. Tree mortality response to drought-density interactions suggests opportunities to enhance drought resistance (Available at:). J. Appl. Ecol. 59 (2), 549–559. https://doi.org/10.1111/1365-2664.14073.

Bradshaw, C.J., Ehrlich, P.R., Beattie, A., Ceballos, G., Crist, E., Diamond, J., Dirzo, R., Ehrlich, A.H., Harte, J., Harte, M.E., 2021. Underestimating the challenges of avoiding a ghastly future (Available at:). Front. Conserv. Sci. 1, 9. https://doi.org/10.3389/fcosc.2020.615419.

Bronson, J., Petrick, J., Danchok, R., 2018. Efficacy of Early Pruning to Reduce the Incidence of White Pine Blister Rust on Sugar Pine (Pinus lambertiana)'. In: Schoettle, A.W., Sniezko, R.A., Kliejunas, J.T. (Eds.), Proceedings of the IUFRO joint conference: Genetics of five-needle pines, rusts of forest trees, and Strobusphere; 2014 June 15-20. Fort Collins, CO. Proc. RMRS-P-76. U.S. Department of Agriculture, Forest Service, Rocky Mountain Research Station, Fort Collins, CO, pp. 205–208 (Available at). ⟨https://www.fs.usda.gov/research/treesearch/56737⟩.

Bürkner, P., Gabry, J., Kay, M. and Vehtari, A. (2021) posterior: Tools for Working with Posterior Distributions. Available at: ⟨https://mc-stan.org/posterior/⟩.

Burrill, E.A., DiTommaso, A.M., Turner, J.A., Pugh, S.A., Christensen, G., Perry, C.J., Conkling, B.L. (2021) Forest Inventory and Analysis Database Description and User Guide for Phase 2 User Guide (version: 9.0), U.S. Forest Service, revision 06.2021. Available at ⟨https://www.fia.fs.usda.gov/library/database-documentation/#FIADB⟩.

California Wildfire & Forest Resilience Task Force. (2023) ⟨https://wildfiretaskforce.org/⟩. Accessed July 4, 2023.

Collins, B.M., Das, A.J., Battles, J.J., Fry, D.L., Krasnow, K.D., Stephens, S.L., 2014. Beyond reducing fire hazard (Available at:). Ecol. Appl. 24 (8), 1879–1886. https://doi.org/10.1890/14-0971.1.

Coop, J.D., et al., 2020. Wildfire-driven forest conversion in western North American landscapes (Available at:). BioScience 70 (8), 659–673. https://doi.org/10.1093/biosci/biaa061.

Das, A., 2012. The effect of size and competition on tree growth rate in old-growth coniferous forests (Available at:). Can. J. For. Res. 42 (11), 1983–1995. https://doi.org/10.1139/x2012-142.

Das, A., Battles, J., Van Mantgem, P.J., Stephenson, N.L., 2008. Spatial elements of mortality risk in old-growth forests (Available at:). Ecology 89 (6), 1744–1756. https://doi.org/10.1890/07-0524.1.

Das, A.J., Battles, J.J., Stephenson, N.L., Van Mantgem, P.J., 2007. The relationship between tree growth patterns and likelihood of mortality: a study of two tree species in the Sierra Nevada (Available at:). Can. J. For. Res. 37 (3), 580–597. https://doi.org/10.1139/X06-262.

Das, A.J., Stephenson, N.L., Flint, A., Das, T., van Mantgem, P.J., 2013. Climatic correlates of tree mortality in water- and energy-limited forests (Available at:). PLoS ONE 8 (7). https://doi.org/10.1371/journal.pone.0069917.

Das, A.J., Stephenson, N.L., Davis, K.P., 2016. Why do trees dies? Characterizing the drivers of background tree mortality (Available at:). Ecology 97 (10), 2616–2627. https://doi.org/10.1002/ecy.1497.

Davis, K.T., Dobrowski, S.Z., Higuera, P.E., Holden, Z.A., Veblen, T.T., Rother, M.T., Parks, S.A., Sala, A., Maneta, M.P., 2019. Wildfires and climate change push low-elevation forests across a critical climate threshold for tree regeneration (Available at:). Proc. Natl. Acad. Sci. USA 116 (13), 6193–6198. https://doi.org/10.1073/pnas.1815107116.

Davis, R.S., Hood, S., Bentz, B.J., 2012. Fire-injured ponderosa pine provide a pulsed resource for bark beetles (Available at:). Can. J. For. Res. -Rev. Can. De. Rech. For. 42 (12), 2022–2036. https://doi.org/10.1139/x2012-147.

Doak, D.F., Waddle, E., Langendorf, R.E., Louthan, A.M., Isabelle Chardon, N., Dibner, R. R., Keinath, D.A., Lombardi, E., Steenbock, C., Shriver, R.K., Linares, C., Begoña Garcia, M., Funk, W.C., Fitzpatrick, S.W., Morris, W.F., Peterson, M.L., 2021. A critical comparison of integral projection and matrix projection models for demographic analysis (Available at:). Ecol. Monogr. 91 (2). https://doi.org/10.1002/ecm.1447.

Dudney, J., Willing, C.E., Das, A.J., Latimer, A.M., Nesmith, J.C.B., Battles, J.J., 2021. Nonlinear shifts in infectious rust disease due to climate change (Available at:). Nat. Commun. 12 (1). https://doi.org/10.1038/s41467-021-25182-6.

Dudney, J.C., Nesmith, J.C.B., Cahill, M.C., Cribbs, J.E., Duriscoe, D.M., Das, A.J., Stephenson, N.L., Battles, J.J., 2020. Compounding effects of white pine blister rust, mountain pine beetle, and fire threaten four white pine species (Available at:). Ecosphere 11 (October), e03263. https://doi.org/10.1002/ecs2.3263.

Dunnington, D. (2021) ggspatial: Spatial Data Framework for ggplot2. Available at: ⟨https://cran.r-project.org/package=ggspatial⟩.

Eitzel, M., Battles, J., York, R., Knape, J., De Valpine, P., 2013. Estimating tree growth from complex forest monitoring data (Available at:). Ecol. Appl. 23 (6), 1288–1296. https://doi.org/10.1890/12-0504.1.

Eitzel, M.V., Battles, J., York, R., De Valpine, P., 2015. Can't see the trees for the forest: complex factors influence tree survival in a temperate second growth forest (Available at:). Ecosphere 6 (11), 1–17. https://doi.org/10.1890/ES15-00105.1.

Fettig, C.J., Mortenson, L.A., Bulaon, B.M., Foulk, P.B., 2019. Tree mortality following drought in the central and southern Sierra Nevada, California, U.S (Available at:). For. Ecol. Manag. 432 (August 2018), 164–178. https://doi.org/10.1016/j.foreco.2018.09.006.

Foster, D.E., Battles, J.J., Collins, B.M., York, R.A., Stephens, S.L., 2020. Potential wildfire and carbon stability in frequent-fire forests in the Sierra Nevada: trade-offs from a long-term study (Available at:). Ecosphere 11 (8). https://doi.org/10.1002/ecs2.3198.

Fowells, H.A., Schubert, G.H., 1956. Seed crops of forest trees in the pine region of California'. Technical Bulletin 1150. USDA,, Washington, DC, p. 48 p. (Available at). ⟨https://www.fs.usda.gov/research/treesearch/41063⟩.

Furniss, T.J., Larson, A.J., Kane, V.R., Lutz, J.A., 2018. Multi-scale assessment of post-fire tree mortality models (p. in press. Available at:). Int. J. Wildland Fire. https://doi.org/10.1071/WF18031.

Furniss, T.J., Das, A.J., Mantgem, P.J., Stephenson, N.L., Lutz, J.A., 2021. Crowding, climate, and the case for social distancing among trees (Available at:). Ecol. Appl. (June 2021), 1–14. https://doi.org/10.1002/eap.2507.

Gabry, J. and Mahr, T. (2021) bayesplot: Plotting for BAyesian Models. Available at: ⟨https://mc-stan.org/bayesplot/⟩.

Gabry, J., Češnovar, R., Bales, B., Morris, M., Popov, M., Lawrence, M., Michael Landau, W. and Socolar, J. (2022) cmdstanr. Available at: ⟨https://github.com/stan-dev/cmdstanr/⟩.

Geils, B.W., Hummer, K.E., Hunt, R.S., 2010. White pines, ribes, and blister rust: a review and synthesis (Available at:). For. Pathol. 40 (3–4), 147–185. https://doi.org/10.1111/j.1439-0329.2010.00654.x.

Hessburg, P.F., Spies, T.A., Perry, D.A., Skinner, C.N., Taylor, A.H., Brown, P.M., Stephens, S.L., Larson, A.J., Churchill, D.J., Povak, N.A., Singleton, P.H., McComb, B., Zielinski, W.J., Collins, B.M., Salter, R.B., Keane, J.J., Franklin, J.F., Riegel, G., 2016. Tamm Review: Management of mixed-severity fire regime forests in Oregon, Washington, and Northern California (Available at:). For. Ecol. Manag. 366, 221–250. https://doi.org/10.1016/j.foreco.2016.01.034.

Hicke, J.A., Johnson, M.C., Hayes, J.L., Preisler, H.K., 2012. Effects of bark beetle-caused tree mortality on wildfire (Available at:). For. Ecol. Manag. 271, 81–90. https://doi.org/10.1016/j.foreco.2012.02.005.

Hijmans, R.J. (2021) raster: Geographic Data Analysis and Modeling. Available at: ⟨https://cran.r-project.org/package=raster⟩.

Hood, S.M., McHugh, C.W., Ryan, K.C., Reinhardt, E., Smith, S.L., 2007. Evaluation of a post-fire tree mortality model for western USA conifers (Available at:). Int. J. Wildland Fire 16 (6), 679–689. https://doi.org/10.1071/WF06122.

Hood, S.M., Smith, S.L., Cluck, D.R., 2010. Predicting mortality for five California conifers following wildfire (Available at:). For. Ecol. Manag. 260 (5), 750–762. https://doi.org/10.1016/j.foreco.2010.05.033.

Hood, S.M., Schaupp, W.C., Goheen, D.J., 2022. Radial thinning ineffective at increasing large sugar pine survival (Available at:). For. Ecol. Manag. 520 (9). https://doi.org/10.1016/j.foreco.2022.120351.

IUCN (2022). The IUCN Red List of Threatened Species. Version 2022–2. ⟨https://www.iucnredlist.org/search?query=sugar%20pine&searchType=species⟩. Accessed on: 8/4/2023.

Kinloch Jr., B.B., Scheuner, W.H., 1990. Pinus lambertiana Dougl. In: Burns, R.M., Honkala, B.H. (Eds.), Silvics of North America Vol. 1: Conifers. Agriculture Handbook 654. U.S. Department of Agriculture, Forest Service, Washington, D.C., pp. 370–380 (Available at). ⟨https://www.fs.usda.gov/research/treesearch/1547⟩

Kinloch Jr., B.B., Marosy, M., Huddleston, M.E. (Eds.), 1996. Sugar pine: status, values, and roles in ecosystems: Proceedings of a symposium presented by the California Sugar Pine Management Committee, March 30 - April 1, 1992. University of California. Division of Agriculture and Natural Resources, Davis, CA. Publication 3362. Available at: ⟨https://books.google.com/books?id=VwRj7T5-kNEC&printsec=frontcover&source=gbs_ge_summary_r&cad=0#v=onepage&q&f=false⟩.

Kinloch, Jr., B.B., Sniezko, R.A., Savin, D.P., Danchok, R. and Kegley, A. (2018) Patterns of Variation in Blister Rust Resistance in Sugar Pine (Pinus lambertiana), in *Schoettle*, Anna W.; Sniezko, Richard A.; Kliejunas, John T., *eds. 2018. Proceedings of the IUFRO joint conference: Genetics of five-needle pines, rusts of forest trees, and Strobusphere; 2014 June 15–20; Fort Collins, CO. Proc. RMRS-P-76. Fort Collins, CO* , pp. 124–128.

Kohyama, T.S., Kohyama, T.I., Sheil, D., 2018. Definition and estimation of vital rates from repeated censuses: Choices, comparisons and bias corrections focusing on trees (Available at:). Methods Ecol. Evol. 9 (4), 809–821. https://doi.org/10.1111/2041-210X.12929.

Kress, W.J., Krupnick, G.A., 2022. Lords of the biosphere: Plant winners and losers in the Anthropocene (Available at:). Plants People Planet 4 (4), 350–366. https://doi.org/10.1002/ppp3.10252.

Latham, P., Tappeiner, J., 2002. Response of old-growth conifers to reduction in stand density in western Oregon forests (Available at:). Tree Physiol. 22 (2–3), 137–146. https://doi.org/10.1093/treephys/22.2-3.137.

Levine, C.R., Krivak-Tetley, F., van Doorn, N.S., Ansley, J.-A.S., Battles, J.J., 2016. Long-term demographic trends in a fire-suppressed mixed-conifer forest (Available at:). Can. J. For. Res. 46 (5), 745–752. https://doi.org/10.1139/cjfr-2015-0406.

Lutz, J.A., et al., 2018. Global importance of large-diameter trees (Available at:). Glob. Ecol. Biogeogr. 27 (7), 849–864. https://doi.org/10.1111/geb.12747.

Lutz, J.A., Larson, A.J., Freund, J.A., Swanson, M.E., Bible, K.J., 2013. The importance of large-diameter trees to forest structural heterogeneity (Available at:). PLoS ONE 8 (12). https://doi.org/10.1371/journal.pone.0082784.

Lutz, J.A., Struckman, S., Furniss, T.J., Cansler, C.A., Germain, S.J., Yocom, L.L., McAvoy, D.J., Kolden, C.A., Smith, A.M.S., Swanson, M.E., Larson, A.J., 2020. Large-diameter trees dominate snag and surface biomass following reintroduced fire (Available at:). Ecol. Process. 9 (1). https://doi.org/10.1186/s13717-020-00243-8.

Mahalovich, M. and Stritch, L. (2013) Pinus albicaulis. The IUCN Red List of Threatened Species 2013. Available at: ⟨https://dx.doi.org/10.2305/IUCN.UK.2013–1.RLTS.T39049A2885918.en⟩.

Maloney, P.E., 2011. Incidence and distribution of white pine blister rust in the high-elevation forests of California (Available at:). For. Pathol. 41 (4), 308–316. https://doi.org/10.1111/j.1439-0329.2011.00732.x.

Maloney, P.E., 2014. The multivariate underpinnings of recruitment for three Pinus species in montane forests of the Sierra Nevada, USA (Available at:). Plant Ecol. 215 (2), 261–274. https://doi.org/10.1007/s11258-013-0295-6.

Maloney, P.E., Vogler, D.R., Eckert, A.J., Jensen, C.E., Neale, D.B., 2011. Population biology of sugar pine (Pinus lambertiana Dougl.) with reference to historical disturbances in the Lake Tahoe Basin: implications for restoration (Available at:). For. Ecol. Manag. 262 (5), 770–779. https://doi.org/10.1016/j.foreco.2011.05.011.

van Mantgem, P.J., Stephenson, N.L., 2007. Apparent climatically induced increase of tree mortality rates in a temperate forest (Available at:). Ecol. Lett. 10 (10), 909–916. https://doi.org/10.1111/j.1461-0248.2007.01080.x.

van Mantgem, P.J., Stephenson, N.L., Keifer, M.B., Keeley, J., 2004. Effects of an introduced pathogen and fire exclusion on the demography of sugar pine (Available at:). Ecol. Appl. 14 (5), 1590–1602. https://doi.org/10.1890/03-5109.

van Mantgem, P.J., Stephenson, N.L., Keeley, J.E., 2006. Forest reproduction along a climatic gradient in the Sierra Nevada, California (Available at:). For. Ecol. Manag. 225 (1–3), 391–399. https://doi.org/10.1016/j.foreco.2006.01.015.

van Mantgem, P.J., Stephenson, N.L., Knapp, E., Battles, J., Keeley, J.E., 2011. Long-term effects of prescribed fire on mixed conifer forest structure in the Sierra Nevada, California (Available at:). For. Ecol. Manag. 261 (6), 989–994. https://doi.org/10.1016/j.foreco.2010.12.013.

van Mantgem, P.J., Caprio, A.C., Stephenson, N.L., Das, A.J., 2016. Does prescribed fire promote resistance to drought in low elevation forests of the Sierra Nevada, California, USA? (Available at:). Fire Ecol. 12 (1), 5–15. https://doi.org/10.4996/fireecology.1201013.

van Mantgem, P.J., Falk, D.A., Williams, E.C., Das, A.J., Stephenson, N.L., 2018. Pre-fire drought and competition mediate post-fire conifer mortality in western U.S. National Parks (Available at:). Ecol. Appl. 28 (7), 1730–1739. https://doi.org/10.1002/eap.1778.

van Mantgem, P.J., Falk, D.A., Williams, E.C., Das, A.J., Stephenson, N.L., 2020. The influence of pre-fire growth patterns on post-fire tree mortality for common conifers in western US parks (Available at:). Int. J. Wildland Fire 29 (6), 513–518. https://doi.org/10.1071/WF19020.

Marcille, K.C., Morgan, T.A., McIver, C.P., Christensen, G.A. (2020) California's forest products industry and timber harvest, 2016, Gen. Tech. Rep. PNW-GTR-994. U.S. Department of Agriculture, Forest Service, Pacific Northwest Research Station. 58 p.

McCauley, L.A., Bradford, J.B., Robles, M.D., Shriver, R.K., Woolley, T.J., Andrews, C.A., 2022. Landscape-scale forest restoration decreases vulnerability to drought mortality under climate change in southwest USA ponderosa forest (Available at:). For. Ecol. Manag. 509 (February), 120088. https://doi.org/10.1016/j.foreco.2022.120088.

McElreath, R., 2016, 2016 Statistical Rethinking: A Bayesian Course with Examples in R and STAN, 1st ed..,. Chapman and Hall / CRC,, New York, NY. ISBN 9781315372495. Available at: ⟨https://xcelab.net/rm/statistical-rethinking/⟩.

Merow, C., Dahlgren, J.P., Metcalf, C.J.E., Childs, D.Z., Evans, M.E.K., Jongejans, E., Record, S., Rees, M., Salguero-Gómez, R., Mcmahon, S.M., 2014. Advancing population ecology with integral projection models: a practical guide (Available at:). Methods Ecol. Evol. 5 (2), 99–110. https://doi.org/10.1111/2041-210X.12146.

Millar, C.I., Stephenson, N.L., Stephens, S.L., 2007. Climate change and forests of the future: managing in the face of uncertainty. Ecological applications 17 (8), 2145–2151.

Moran, E.V., Das, A.J., Keeley, J.E., Stephenson, N.L., 2019. Negative impacts of summer heat on Sierra Nevada tree seedlings (Available at:). Ecosphere 10 (6). https://doi.org/10.1002/ecs2.2776.

Morgan, T.A., Brandt, J.P., Songster, K.E., Keegan, C.E., III, Christensen, G.A. (2012) California's forest products industry and timber harvest, 2006, Gen. Tech. Rep. PNW-GTR-866. U.S. Department of Agriculture, Forest Service, Pacific Northwest Research Station. 48 p.

Mullen, L.A., Bratt, J., 2018. USAboundaries: historical and contemporary boundaries of the United States of America (Available at:). J. Open Source Softw. 3 (23), 314. https://doi.org/10.21105/joss.00314.

Müller, K. (2020) here: A Simpler Way to Find Your Files. Available at: ⟨https://cran.r-project.org/package=here⟩.

Müller, K., Wickham, H., James, D.A. and Falcon, S. (2021) RSQLite: "SQLite" Interface for R. Available at: ⟨https://cran.r-project.org/package=RSQLite⟩.

Murray, M.P., Tomback, D.F., 2010. Clark's nutcrackers harvest sugar pine seeds from cones (Available at:). West. North Am. Nat. 70 (3), 413–414. https://doi.org/10.3398/064.070.0314.

NatureServe (2023) 'Sugar Pine.' ⟨https://explorer.natureserve.org/Taxon/ELEMENT_GLOBAL.2.161150/Pinus_lambertiana⟩. Accessed on: 8/4/2023.

Needham, J., Merow, C., Chang-Yang, C.H., Caswell, H., McMahon, S.M., 2018. Inferring forest fate from demographic data: from vital rates to population dynamic models (Available at:). Proc. R. Soc. B: Biol. Sci. 285 (1874). https://doi.org/10.1098/rspb.2017.2050.

Nesmith, J.C.B., O'Hara, K.L., van Mantgem, P.J., de Valpine, P., 2010. The effects of raking on sugar pine mortality following prescribed fire in sequoia and kings canyon national parks, California, USA (Available at:). Fire Ecol. 6 (3), 97–116. https://doi.org/10.4996/fireecology.0603097.

Nesmith, J.C.B., Das, A.J., O'Hara, K.L., van Mantgem, P.J., 2015. The influence of prefire tree growth and crown condition on postfire mortality of sugar pine following prescribed fire in Sequoia National Park (Available at:). Can. J. For. Res. 45 (7), 910–919. https://doi.org/10.1139/cjfr-2014-0449.

Newman, E.A., 2019. Disturbance ecology in the anthropocene (Available at:). Front. Ecol. Evol. 7, 147. https://doi.org/10.3389/fevo.2019.00147.

Niinemets, Ü., Valladares, F., 2006. Tolerance to shade, drought, and waterlogging of temperate northern hemisphere trees and shrubs (Available at). Ecol. Monogr. 76 (4), 521–547. https://doi.org/10.1890/0012-9615(2006)076[0521:TTSDAW]2.0.CO;2.

North, M.P., et al., 2019. Tamm review: reforestation for resilience in dry western U.S. forests (Available at:). For. Ecol. Manag. 432 (July 2018), 209–224. https://doi.org/10.1016/j.foreco.2018.09.007.

North, M.P., York, R.A., Collins, B.M., Hurteau, M.D., Jones, G.M., Knapp, E.E., Kobziar, L., Mccann, H., Meyer, M.D., Stephens, S.L., Tompkins, R.E., Tubbesing, C. L., 2021. Pyrosilviculture needed for landscape resilience of dry western United States forests (Available at:). J. For. 1–25. https://doi.org/10.1093/jofore/fvab026.

North, M.P., Tompkins, R.E., Bernal, A.A., Collins, B.M., Stephens, S.L., York, R.A., 2022. Operational resilience in western US frequent-fire forests (Available at:). For. Ecol. Manag. 507 (November 2021), 120004. https://doi.org/10.1016/j.foreco.2021.120004.

Ohse, B., Compagnoni, A., Farrior, C.E., McMahon, S.M., Salguero-Gómez, R., Rüger, N., Knight, T.M., 2023. Demographic synthesis for global tree species conservation (Available at:). Trends Ecol. Evol. 38 (6). https://doi.org/10.1016/j.tree.2023.01.013.

Parks, S.A., Abatzoglou, J.T., 2020. Warmer and drier fire seasons contribute to increases in area burned at high severity in western US forests from 1985 to 2017 (Available at:). Geophys. Res. Lett. 47 (22), 1–10. https://doi.org/10.1029/2020GL089858.

Paz-Kagan, T., Brodrick, P.G., Vaughn, N.R., Das, A.J., Stephenson, N.L., Nydick, K.R., Asner, G.P., 2017. What mediates tree mortality during drought in the southern Sierra Nevada (Available at:). Ecol. Appl. 27 (8), 2443–2457. https://doi.org/10.1002/eap.1620.

Pebesma, E., 2018. Simple features for R: standardized support for spatial vector data (Available at:). R. J. 10 (1), 439–446. https://doi.org/10.32614/rj-2018-009.

Pebesma, E., Mailund, T., Hiebert, J., 2016. Measurement units in R (Available at:). R. J. 8 (2), 490–498. https://doi.org/10.32614/rj-2016-061.

R Core Team, 2021. R: A language and environment for statistical computing. R Foundation for Statistical Computing,, Vienna, Austria (Available at). ⟨https://www.r-project.org⟩.

Restaino, C., Young, D.J.N., Estes, B., Gross, S., Wuenschel, A., Meyer, M., Safford, H., 2019. Forest structure and climate mediate drought-induced tree mortality in forests of the Sierra Nevada, USA (Available at:). Ecol. Appl. 29 (December 2017), 1–14. https://doi.org/10.1002/eap.1902.

Rivers, M., Newton, A.C., Oldfield, S., Global Tree Assessment Contributors, 2023. Scientists' warning to humanity on tree extinctions (Available at:). Plants, People, Planet 5, 466–482. https://doi.org/10.1002/ppp3.10314.

R-SIG-DB, Wickham, H. and Müller, K. (2021) DBI: R Database Interface. Available at: ⟨https://cran.r-project.org/package=DBI⟩.

Safford, H.D., Stevens, J.T., 2017. Natural Range of Variation (NRV) for yellow pine and mixed conifer forests in the bioregional assessment area, including the Sierra Nevada, southern Cascades, and Modoc and Inyo National Forests. Gen. Tech. Rep. PSW-GTR-2562 (October), 1–151.

Schubert, G.H., 1956. Effect of fertilizer on cone production of sugar pine. Res. Note 116. USDA Forest Service, California Forest and Range Experiment Station,, Berkeley, CA, p. 4. Available at: ⟨https://www.fs.usda.gov/psw/pubs/60127⟩.

Schwilk, D.W., Ackerly, D.D., 2001. Flammability and serotiny as strategies: correlated evolution in pines evolution correlated as strategies: and serotiny flammability in pines. Oikos 94, 326–336 (Available at). ⟨https://www.jstor.org/stable/3547577⟩.

Scott, C.T., Bechtold, W.A., Reams, G.A., Smith, W.D., Westfall, J.A., Hansen, M.H. and Moisen, G.G. (2005) Chapter 4: Sample-based estimators used by the Forest Inventory and Analysis National Information Management System' in Bechtold, W.A. and Patterson, P.L (compilers). *The Enhanced Forest Inventory and Analysis Program — National Sampling Design and Estimation Procedures*, USDA General Technical Report, SRS-80, p. 85.

Shive, K.L., Preisler, H.K., Welch, K.R., Safford, H.D., Butz, R.J., O'Hara, K.L., Stephens, S.L., 2018. From the stand scale to the landscape scale: predicting the spatial patterns of forest regeneration after disturbance (Available at:). Ecol. Appl. 28 (6), 1626–1639. https://doi.org/10.1002/eap.1756.

Shriver, R.K., Andrews, C.M., Arkle, R.S., Barnard, D.M., Duniway, M.C., Germino, M.J., Pilliod, D.S., Pyke, D.A., Welty, J.L., Bradford, J.B., 2019. Transient population dynamics impede restoration and may promote ecosystem transformation after disturbance (Available at:). Ecol. Lett. 22 (9), 1357–1366. https://doi.org/10.1111/ele.13291.

Shriver, R.K., Yackulic, C.B., Bell, D.M., Bradford, J.B., 2021. Quantifying the demographic vulnerabilities of dry woodlands to climate and competition using range-wide monitoring data (Available at:). Ecology 102 (8), 1–12. https://doi.org/10.1002/ecy.3425.

Sniezko, R.A., Liu, J.J., 2022. Genetic resistance to white pine blister rust, restoration options, and potential use of biotechnology (Available at:). For. Ecol. Manag. 520, 120168. https://doi.org/10.1016/j.foreco.2022.120168.

Spies, T.A., Lindenmayer, D.B., Gill, A.M., Stephens, S.L., Agee, J.K., 2012. Challenges and a checklist for biodiversity conservation in fire-prone forests: perspectives from the Pacific Northwest of USA and Southeastern Australia (Available at:). Biol. Conserv. 145, 5–14. https://doi.org/10.1016/j.biocon.2011.09.008.

Stan Development Team (2022) Stan Modeling Language Users Guide and Reference Manual'. Available at: ⟨https://mc-stan.org⟩.

Stanke, H., Finley, A.O., Weed, A.S., Walters, B.F., Domke, G.M., 2020. rFIA: an R package for estimation of forest attributes with the US forest inventory and analysis database (Available at). Environ. Model. Softw. 127, 104664. https://doi.org/10.1016/j.envsoft.2020.104664.

Steel, Z.L., Safford, H.D., Viers, J.H., 2015. The fire frequency-severity relationship and the legacy of fire suppression in California forests. http://www.esajournals.org/doi/pdf/10.1890/ES14-00224.1 Ecosphere 6 (1). https://doi.org/10.1890/ES14-00224.1.

Steel, Z.L., Goodwin, M., Meyer, M., Fricker, G.A., Zald, H., Hurteau, M.D., 2021. Do forest fuel reduction treatments confer resistance to beetle infestation and drought mortality? (Available at:). Ecosphere 12 (January). https://doi.org/10.1002/ecs2.3344.

Stephens, S.L., Moghaddas, J.J., 2005. Experimental fuel treatment impacts on forest structure, potential fire behavior, and predicted tree mortality in a California mixed conifer forest (Available at:). For. Ecol. Manag. 215 (1–3), 21–36. https://doi.org/10.1016/j.foreco.2005.03.070.

Stephens, S.L., Moghaddas, J.J., Edminster, C., Fiedler, C.E., Haase, S., Harrington, M., Keeley, J.E., Knapp, E.E., McIver, J.D., Metlen, K., Skinner, C.N., Youngblood, A., 2009. Fire treatment effects on vegetation structure, fuels, and potential fire severity in Western U. S. forests (Available at:). Ecol. Appl. 19 (2), 305–320. https://doi.org/10.1890/07-1755.1.

Stephens, S.L., Lydersen, J., Collins, B.M., Fry, D., 2015. Historical and current landscape-scale ponderosa pine and mixed conifer forest structure in the Southern Sierra Nevada. Ecosphere 6 (May), 1–63.

Stephens, S.L., Collins, B.M., Fettig, C.J., Finney, M.A., Hoffman, C.M., Knapp, E.E., North, M.P., Safford, H., Wayman, R.B., 2018. Drought, tree mortality, and wildfire in forests adapted to frequent fire (Available at:). BioScience 68 (2), 77–88. https://doi.org/10.1093/biosci/bix146.

Stephenson, N.L., 1998. Actual evapotranspiration and deficit: biologically meaningful correlates of vegetation distribution across spatial scales (Available at:). J. Biogeogr. 25 (5), 855–870. https://doi.org/10.1046/j.1365-2699.1998.00233.x.

Stephenson, N.L., Das, A.J., Ampersee, N.J., Bulaon, B.M., Yee, J.L., 2019. Which trees die during drought? The key role of insect host-tree selection (Available at:). J. Ecol. 107 (5), 2383–2401. https://doi.org/10.1111/1365-2745.13176.

Stevens, J.T., Collins, B.M., Miller, J.D., North, M.P., Stephens, S.L., 2017. Changing spatial patterns of stand-replacing fire in California conifer forests (Available at:). For. Ecol. Manag. 406 (August), 28–36. https://doi.org/10.1016/j.foreco.2017.08.051.

Stevens, K.A., Wegrzyn, J.L., Zimin, A., Puiu, D., Crepeau, M., Cardeno, C., Paul, R., Gonzalez-Ibeas, D., Koriabine, M., Holtz-Morris, A.E., 2016. Sequence of the sugar pine megagenome (Available at:). Genetics 204 (4), 1613–1626. https://doi.org/10.1534/genetics.116.193227.

Stewart, J.A.E., van Mantgem, P.J., Young, D.J.N., Shive, K.L., Preisler, H.K., Das, A.J., Stephenson, N.L., Keeley, J.E., Safford, H.D., Wright, M.C., Welch, K.R., Thorne, J. H., 2021. Effects of postfire climate and seed availability on postfire conifer regeneration (Available at:). Ecol. Appl. 31 (3), 1–14. https://doi.org/10.1002/eap.2280.

Tennekes, M., 2018. Tmap: thematic maps in R (Available at:). J. Stat. Softw. 84 (6). https://doi.org/10.18637/jss.v084.i06.

Thayer, T.C., Wall, S.B.Vander, Journal, S., Mar, N., 2005. Interactions between Steller's jays and yellow pine chipmunks over scatter-hoarded sugar pine seeds. J. Anim. Ecol. 74 (2), 365–374. ⟨https://www.jstor.org/stable/3505625⟩.

US Fish and Wildlife Service (2020) Endangered and Threatened Wildlife and Plants: Threatened Species Status for Pinus albicaulis (Whitebark Pine) with Section 4(d) Rule, FWS-R6-ES-2019–0054-0001. Available at ⟨https://www.regulations.gov/document/FWS-R6-ES-2019–0054-0001⟩.

Voelker, S.L., Merschel, A.G., Meinzer, F.C., Ulrich, D.E.M., Spies, T.A., Still, C.J., 2019. Fire deficits have increased drought sensitivity in dry conifer forests: fire frequency and tree-ring carbon isotope evidence from Central Oregon (Available at:). Glob. Change Biol. 25 (4), 1247–1262. https://doi.org/10.1111/gcb.14543.

Waring, K.M., Goodrich, B.A., 2012. Artificial regeneration of five-needle pines of western North America: a survey of current practices and future needs. Tree Planters Notes 55 (2), 55–71.

Wayman, R.B., Safford, H.D., 2021. Recent bark beetle outbreaks influence wildfire severity in mixed-conifer forests of the Sierra Nevada, California, USA (Available at:). Ecol. Appl. 31 (3), 1–19. https://doi.org/10.1002/eap.2287.

Western Wood Products Association (1993) *Statistical Yearbook of the Western Lumber Industry:1993*.

Westfall, J.A., Coulston, J.W., Scott, C.T., 2022. Chapter 2: Foundational Documentation. In: Westfall, J.A., Coulston, J.W., Moisen, G.G., Andersen, H.E., compilers (Eds.), Sampling and estimation documentation for the Enhanced Forest Inventory and Analysis Program: 2022. USDA Forest Service. https://doi.org/10.2737/NRS-GTR-207.

Wickham, H., et al., 2019. Welcome to the tidyverse (Available at:). J. Open Source Softw. 4 (43), 1686. https://doi.org/10.21105/joss.01686.

Wilke, C.O. (2020) cowplot: Streamline Plot Theme and Plot Annotations for "ggplot2"'. Available at: ⟨https://cran.r-project.org/package=cowplot⟩.

Yeaton, R.I., 1983. The successional replacement of ponderosa pine by sugar pine in the Sierra Nevada (Available at:). Bull. Torre Bot. Club 110 (3), 292–297. https://doi.org/10.2307/2996181.

Yeaton, R.I., 1984. Aspects of the population biology of sugar pine (Pinus lambertiana Dougl.) on an elevational gradient in the Sierra Nevada of Central California. Am. Midl. Nat. 111 (1), 126–137 (Available at). ⟨https://www.jstor.org/stable/2425550⟩.

York, R.A., Heald, R.C., Battles, J.J., York, J.D., 2004. Group selection management in conifer forests: relationships between opening size and tree growth (Available at:). Can. J. For. Res. 34 (3), 630–641. https://doi.org/10.1139/x03-222.

York, R.A., Battles, J.J., Wenk, R.C., Saah, D., 2012. A gap-based approach for regenerating pine species and reducing surface fuels in multi-aged mixed conifer stands in the Sierra Nevada, California (Available at:). Forestry 85 (2), 203–213. https://doi.org/10.1093/forestry/cpr058.

Young, D.J.N., Stevens, J.T., Earles, J.M., Moore, J., Ellis, A., Jirka, A.L., Latimer, A.M., 2017. Long-term climate and competition explain forest mortality patterns under extreme drought (Available at:). Ecol. Lett. 20 (1), 78–86. https://doi.org/10.1111/ele.12711.